PHILOSOPHICAL TRANSACTIONS OF THE ROYAL SOCIETY A MATHEMATICAL, PHYSICAL & ENGINEERING SCIENCES

Splashing of Water Drops on Solid and Wetted Surfaces: Hydrodynamics and Charge Separation

Z. Levin and P. V. Hobbs

Phil. Trans. R. Soc. Lond. A 1971 **269**, 555-585
doi: 10.1098/rsta.1971.0052

SPLASHING OF WATER DROPS ON SOLID AND WETTED SURFACES: HYDRODYNAMICS AND CHARGE SEPARATION

By Z. Levin and P. V. Hobbs
Atmospheric Sciences Department, University of Washington, Seattle, Washington, U.S.A.

(*Communicated by Sir Geoffrey Taylor, O.M., F.R.S.—Received* 1 *December* 1970—*Read* 29 *April* 1971)

[Plates 13 to 16]

CONTENTS

The charges separated by splashes on solid and wetted surfaces are shown to be carried on the liquid fragments ejected from the crown. Experimental observations on the nature of these splashes are presented and mechanisms for the formation and break-up of the crown are proposed. The surface on which a splash occurs is generally left with a positive charge, the magnitude of which decreases with increasing concentration of solute in the drop. This is explained by the disruption of the electrical double layer. When drops containing ammonium hydroxide in excess of 2.5×10^{-5} mol l^{-1} splash on ice at -1 °C the ice receives a positive charge. In this case, freezing potentials appear to play a role in the charging. In an applied electric field the charges separated by splashing increase as the field is increased, in agreement with an induction mechanism of charging. Also, in an applied electric field, the charges initially increase as the impact speed is increased but beyond a certain impact speed the charges decrease. This is explained in terms of the relative magnitudes of the time of contact of the ejected liquid fragments with the crown and the relaxation time of charge carriers in the liquid.

The role of charge separation due to splashing in thunderstorm electrification and in the build-up of space charges during rainfall is discussed.

Vol. 269. A. 1200. (Price £1.10; U.S. $2.85) 45 [Published 13 May 1971

1. Introduction

The break-up of liquids under various conditions has been studied by many workers since the middle of the nineteenth century. Some of these investigations have dealt with the hydrodynamics of the break-up, while others have been more concerned with the electrical charges separated by the disintegration of the liquid. These studies, in addition to being of inherent interest, have important applications to such problems as soil erosion, erosion in steam turbines by water drops, damage to aircraft by raindrops, and atmospheric electricity.

The main objective of the work described in this paper was to study the separation of electrical charges produced by the splashing of water drops on solid surfaces and into thin layers of water. However, the charges separated by splashing are intimately connected with the nature of the splash itself. In the following section, therefore, we consider the hydrodynamics of splashing onto solid surfaces and into thin layers of liquid. In §3 the results of an investigation into the charges separated by splashes of this kind are described. Finally, in §4 the role of splashing in separating electrical charges in the atmosphere is considered briefly.

2. The hydrodynamics

2.1. *General features of splashes*

Most studies of splashing have been concerned with the impact of drops on deep liquids. In this case, as shown by the original work of Worthington & Cole (1897, 1900), the following sequence of events takes place. After the drop has collided with the surface a flared film of liquid is thrown upward and outward from the periphery of the drop. The height of this film increases as the drop penetrates further into the liquid and small jets of liquid are shot out from the upper rim of the film giving it the appearance of a crown. These jets break up into numerous small liquid fragments. At the same time, the cavity which forms beneath the surface of the liquid, due to the impact of the drop, is enlarged. As the wall of the crown begins to subside and thicken, the cavity collapses. The combined effects of the collapse of the cavity and the subsidence of the crown cause a relatively large column of liquid, known as the Rayleigh jet, to rise above the surface. The Rayleigh jet may pinch off to form one or more large drops.

As the depth of the liquid into which the drop splashes is decreased the features of the splash described above undergo changes (Hobbs & Osheroff 1967; Macklin & Hobbs 1969). For example, if a drop of liquid water 2.3 mm in diameter falls through a distance of 75 cm in air before it impacts on liquid water, the crown that is formed becomes increasingly unstable as the depth of the water is decreased below about 5 mm. Also, as the depth of the water is decreased from 25 to 7 mm the maximum height to which the Rayleigh jet rises increases and more drops break away from the Rayleigh jet. However, for depths of water less than 7 mm, both the height of the Rayleigh jet and the number of drops which break away from it fall off sharply. No drops break away from the Rayleigh jet for depths of water less than about 3 mm. These variations in the nature of the splash with depth of liquid have been explained by Macklin & Hobbs in terms of the interaction of the subsurface cavity with the solid boundary beneath the shallow liquid.

Studies of splashing on solid surfaces were initiated by Worthington (1876, 1877). He investigated the patterns left by drops of various liquids after they had fallen onto horizontal smoked glass plates. Most of the recent work which has been done on splashing on solid surfaces has

been concerned with the erosion caused by the impact. Consequently, attention has been directed at the pressure developed on impact and the spread of the liquid over the solid surface (Engel 1955; Savic & Boult 1955; Bowden & Field 1964; Bowden & Brunton 1967; Heymann 1969). Comparatively little work has been done on the crown which develops when a drop splashes on solid surfaces. It will be shown later in this paper that the charge separation which takes place when drops splash on solid or wetted surfaces is caused by the break-up of jets which form on the crown. Therefore, the emphasis in our study of the hydrodynamics of splashing was on the crown and its break-up.

2.2. *Experimental*

The interval of time from the initial impact of a drop on a solid surface to the end of the splashing event is of the order of 1 ms. (The corresponding time interval for splashing into liquids is about 10 ms.) Therefore, in order to photograph the sequence of events high-speed photographic techniques must be used.

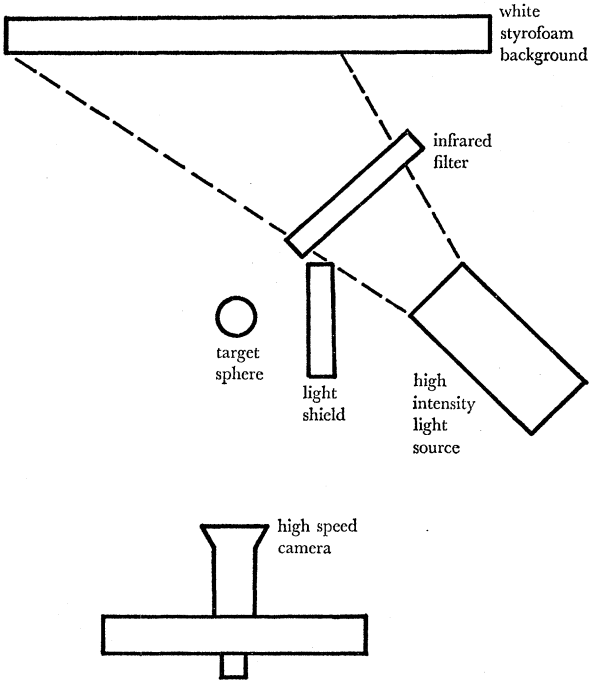

FIGURE 1. Plan view of the experimental arrangement for obtaining high-speed photographs of drop splashing.

A sketch of the experimental arrangement that was used for obtaining these photographs is shown in figure 1. The splash was illuminated by light from a 1 kW lamp reflected from a white styrofoam sheet. The camera was generally operated at speed of about 5000 frames per second and Kodak 4 X negative 16 mm film was used. Drops from about 0.4 to 3 mm in diameter were produced using the technique described by Reil & Hallett (1968). Measurements on individual drops showed that for the larger drops (> 1.2 mm) there was a variation of about 3 % in the diameters, and for the smaller drops a variation of about 8 %. The average diameter of the drops used in any one experiment was determined from the weight of 100 drops. The target generally consisted of a copper hemisphere 2.5 cm in diameter which was either dry or covered with a thin layer of water. In some cases the hemisphere was replaced by an ice sphere of the same radius.

2.3. *Results*

(*a*) *General observations*

Figure 2, plate 13, shows a sequence of photographs of the splash produced by a water drop, 2.94 mm in diameter, after it had fallen through a vertical height of 45 cm and collided with the dry copper hemisphere with an impact velocity of 2.8 m s^{-1}. These photographs reveal the main features of splashing on rough solid surfaces. After impact the liquid flows radially outward from the underside of the drop to form a thin liquid layer on the solid surface, on the periphery of this layer a liquid crown extends upward (figure 2*e*). As the drop collapses, the liquid layer increases in area and the crown increases in height (figure 2*f*). Radial disturbances develop on the growing wall of the crown; these appear as light and dark bands in these photographs (figure 2*f*). As the wall of the crown increases in height long jets of liquid form along its upper periphery (figure 2*g*). These jets become unstable and break up into many small fragments which are shot out from the crown (figure 2*j*) with a high velocity and are thrown a considerable distance. It is clear from the photographs that instabilities develop on the crown before it reaches its maximum height, and these cause many droplets to be thrown off within 0.2 to 0.7 ms after impact. The wall of the crown eventually decreases in height and collapses back onto the surface. We have observed on some occasions that even during the collapse of the wall of the crown jets may form and break up into droplets. However, during this stage the velocities of ejection of the droplets are comparatively small so the droplets do not travel far. It should be noted that a Rayleigh jet is not formed by splashing onto a solid surface. When water drops impact onto a very smooth solid surface a crown is not formed; the drop simply spreads out radially over the surface. The discussion in this paper will be restricted to splashing on comparatively rough solid surfaces and wetted surfaces.

The effect of the speed of impact on splashing on solid surfaces was investigated by allowing the water drops to fall through various distances before colliding with a copper hemisphere. A summary of the results is shown in table 1. The term 'disappearance of drop' in this table refers to the point on which the curvature of the original drop jet disappears (e.g. figure 2*j*), that is, when there is no pressure head of water remaining.

Figure 3 shows how the diameter of the base of the crown varies with time measured from the moment of impact. The diameter initially increases rapidly but then the velocity of spread over the solid surface gradually decreases. It is interesting to compare the speed of impact of the drop on the surface with the radial flow speed of the base of the crown. The latter quantity was obtained at various times from the gradients of the curves in figure 3. Figure 4 shows how the ratio of the radial flow speed to the impact speed varies with time. It can be seen from these results that the initial radial flow speed of the base of the crown is about an order of magnitude greater than the impact speed. This is a consequence of the pressure which builds up in the drop after impact (Engel 1955; Bowden & Field 1964). However, the initial high velocity of spread decays very fast and reaches a value comparable to the impact speed within about 1.1 to 1.5 ms (i.e. before the complete collapse of the drop). Figure 5 shows how the speed at which the top of the drop approaches the solid surface following impact varies with time measured from the moment of impact.

Description of plate 13

Figure 2. Sequence of photographs of the splash produced by a water drop 2.94 mm in diameter which collided with a copper surface with an impact speed of 2.8 m s^{-1}. *t* is time after moment of impact. (Magn. × 4.7.)

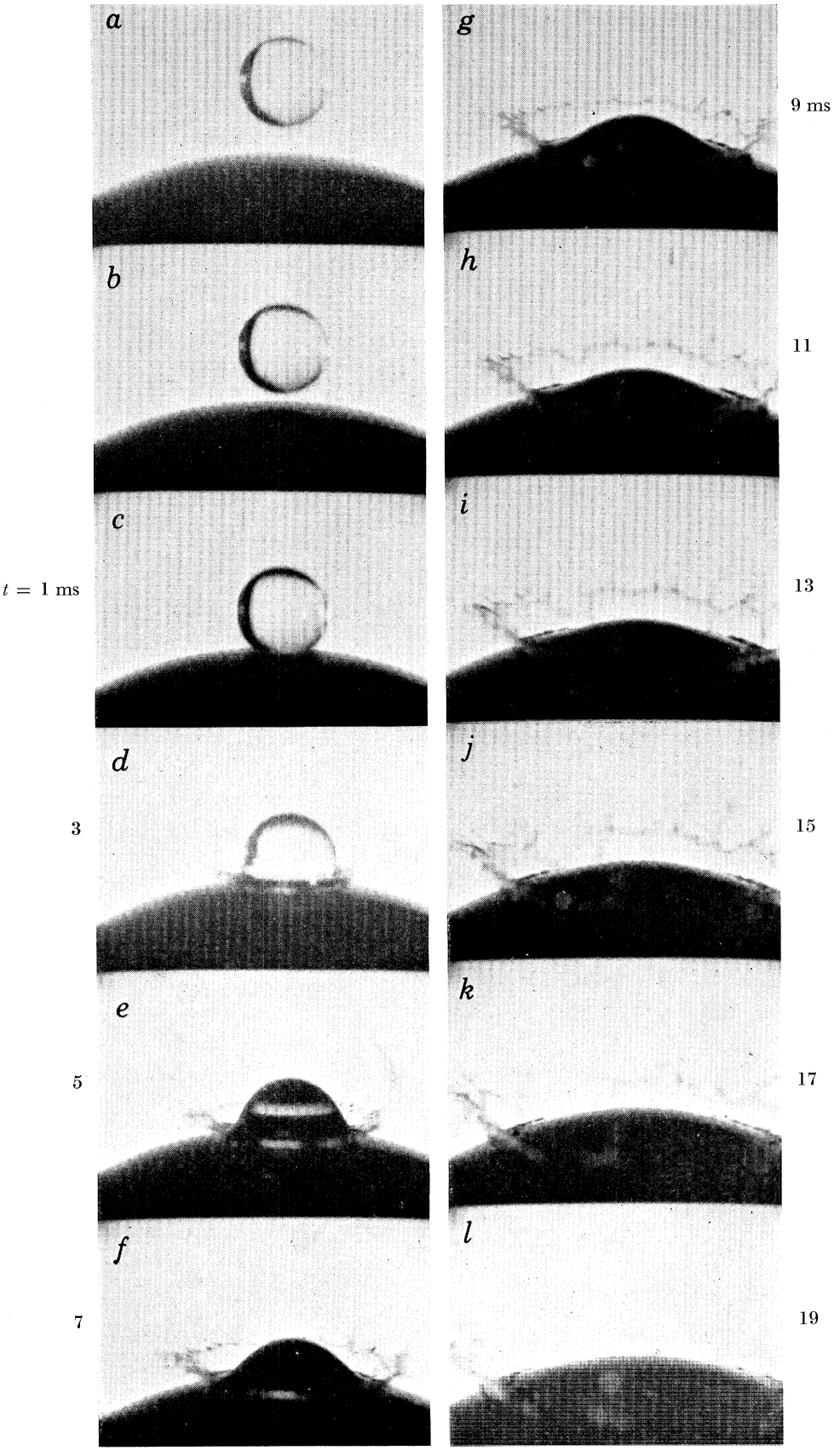

FIGURE 2. For legend see facing page

(*Facing p.* 558)

PHILOSOPHICAL TRANSACTIONS OF THE ROYAL SOCIETY A MATHEMATICAL, PHYSICAL & ENGINEERING SCIENCES

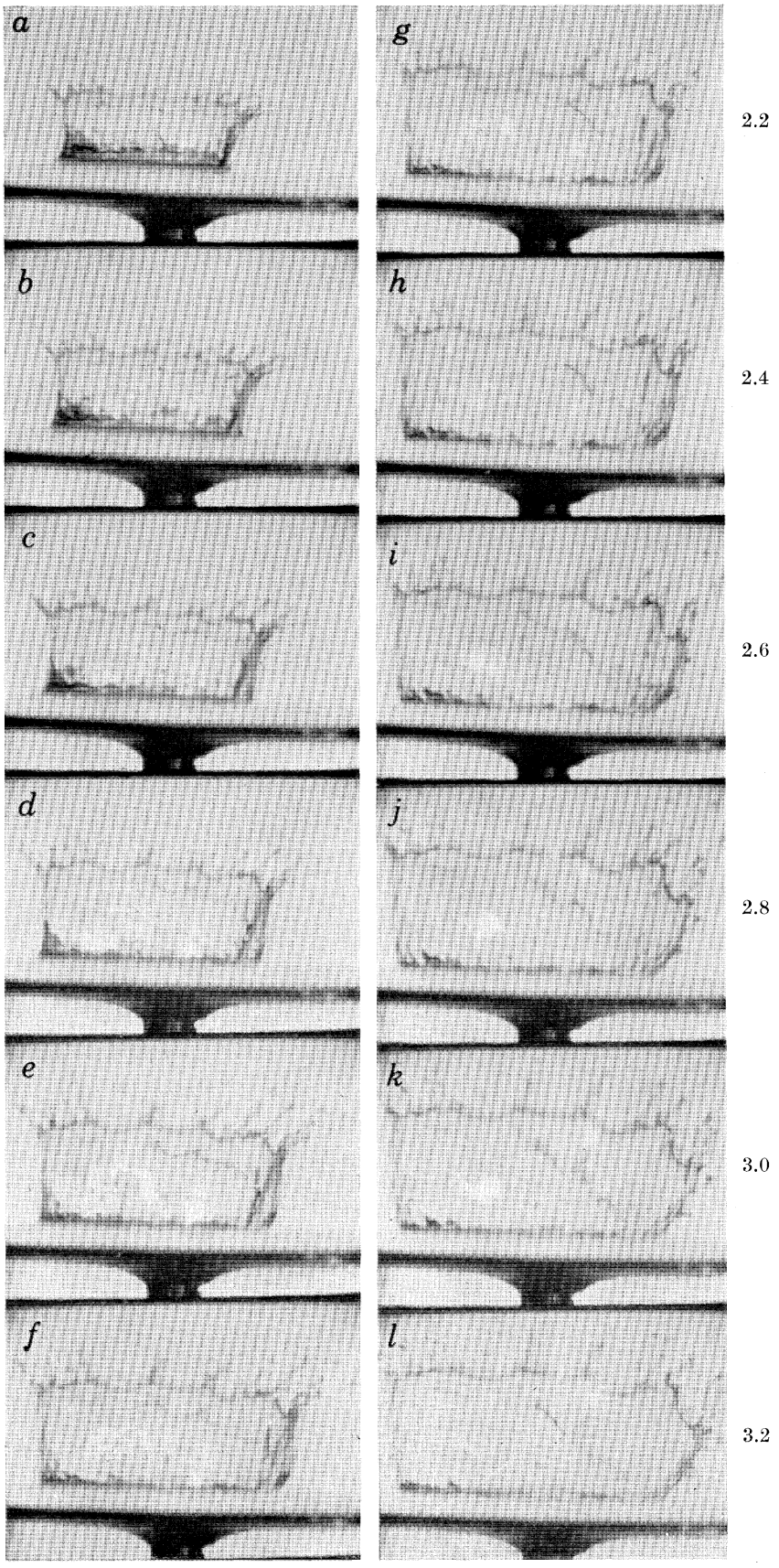

FIGURE 8. For legend see facing page

PHILOSOPHICAL TRANSACTIONS OF THE ROYAL SOCIETY A MATHEMATICAL, PHYSICAL & ENGINEERING SCIENCES

TABLE 1. SUMMARY OF RESULTS ON EFFECT OF IMPACT SPEED ON SPLASHING ONTO A SOLID SURFACE

fall distance/cm...	15	30	45	62	110	145.5
diameter of drop/mm	2.9	2.9	2.9	2.9	2.9	2.9
impact speed/m s^{-1}	1.68	2.13	2.81	3.12	3.95	4.8
time from impact to disappearance of drop†/ ms	2.1	1.8	1.5	1.1	0.95	0.8
diameter of base of crown at time of disappearance of drop†/mm	9.0	8.91	8.87	8.07	9.73	10.6
height of crown at time of disappearance of drop†/mm	0.851	1.38	1.935	1.96	2.0	2.65
maximum height of crown/mm	1.1	1.39	2.19	2.45	2.5	2.65
time for crown to reach maximum height/ms	2.3	1.9	1.7	1.4	1.0	0.9
ratio of height to diameter of crown at time of disappearance of drop†	0.19	0.325	0.438	0.49	0.42	0.5

† See text for definition of 'disappearance of drop'.

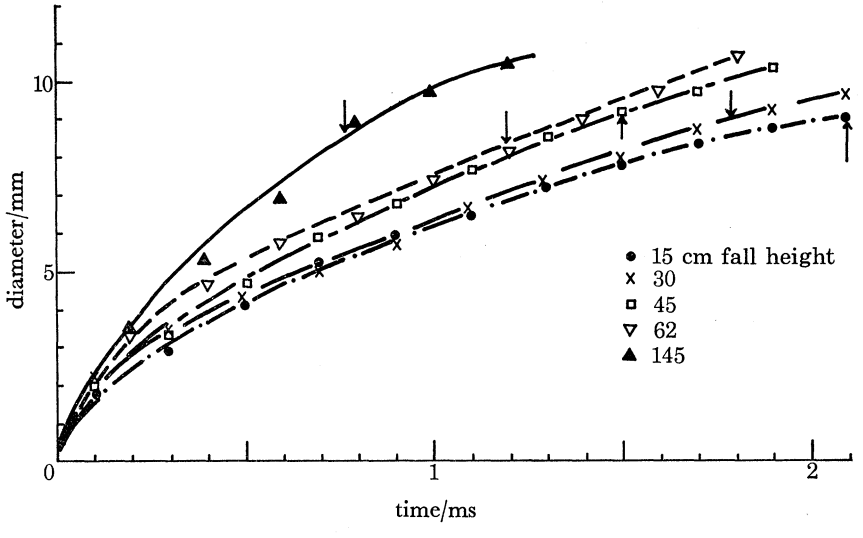

FIGURE 3. Diameter of the base of the crown as a function of time measured from the moment of impact. (Arrow indicates the point at which the drop 'disappeared'.)

DESCRIPTION OF PLATE 14

FIGURE 8. Sequence of photographs of the splash produced by a water drop 2.9 mm in diameter which collided with a layer of water 0.5 mm in depth with an impact speed of 4.8 m s^{-1}. t is time after moment of impact. (Magn. ×2.82.)

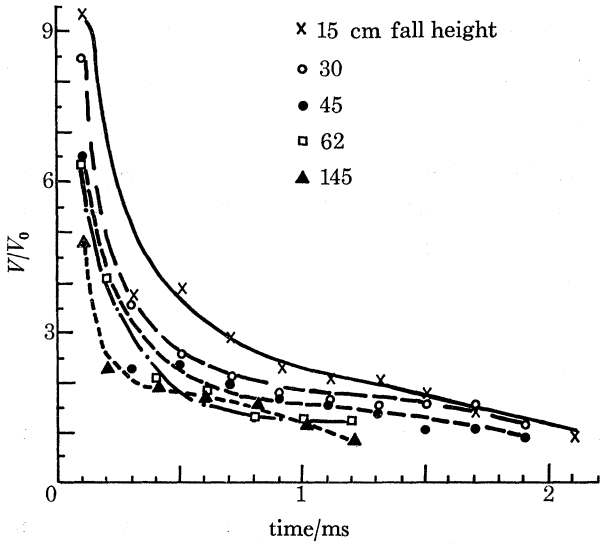

FIGURE 4. Ratio of the radial speed V of the base of the crown to the impact speed V_0 of the drop with the solid surface as a function of time measured from the moment of impact. The drops were 2.94 mm in diameter in each case.

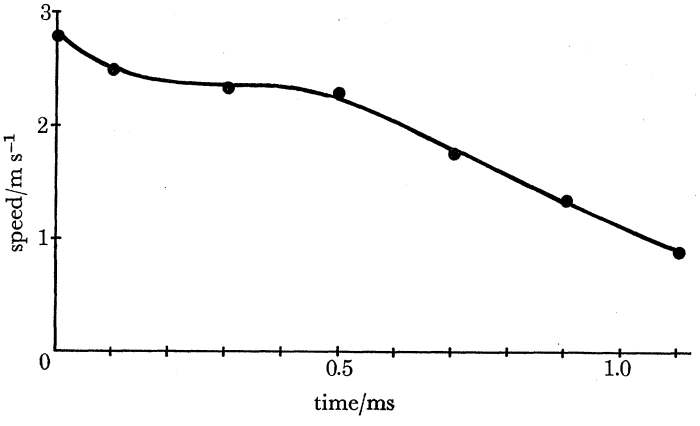

FIGURE 5. Speed at which the top of a drop approaches a solid surface following impact as a function of time measured from the moment of impact. The drop was 2.94 mm in diameter and the impact speed was 2.81 m s^{-1}.

(*b*) *Measurements on the droplets from the crown*

Estimates were made of the number and size distribution of droplets ejected from the crown in the following way. The copper hemisphere was placed on a clear glass plate and water drops 2.50 mm in diameter were allowed to splash onto the hemisphere with an impact speed of 4.2 m s^{-1}. The fragments thrown off from the crown fell onto the glass plate where they were photographed within 10 s of landing. The size distribution of the droplets was then determined by measurements on the photographs under a microscope. This procedure was repeated several times and an average size distribution determined. The results are shown in figure 6. In figure 7 the same results are plotted on log–normal probability paper, the fact that the results fall on a straight line on this plot indicates that the drop size distribution is log–normal. It should be noted, however, that these measurements do not include droplets less than 50 μm in diameter. These droplets, which are ejected from the crown at relatively high velocities, were not collected on the glass plate. Moreover, droplets less than 50 μm in diameter probably evaporate

soon after leaving the crown. To obtain information on these very small droplets, large prints were made from the 16 mm film and carefully examined. They revealed that a large number of droplets less than 50 μm in diameter are ejected from the crown, but it was not possible to count their number directly. However, the photographs showed that about twenty jets form on a crown. If it is assumed that while a jet is initially very narrow it ejects two droplets less than

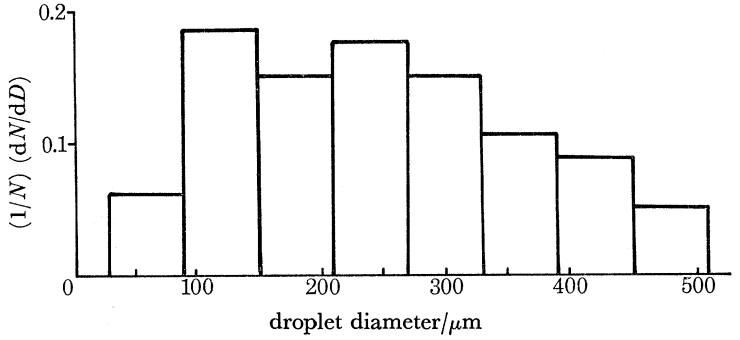

FIGURE 6. Normalized average size distribution of the droplets ejected from the crowns of splashes produced by drops 2.5 mm in diameter after falling a distance of 1.5 m and impacting on a solid surface. Total number of droplets was 110.

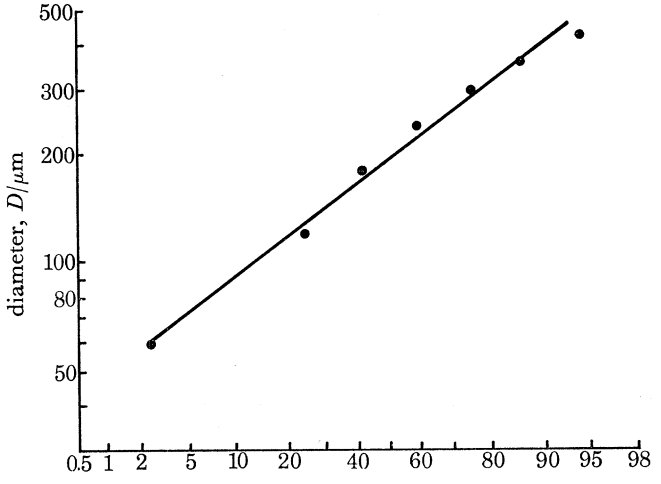

FIGURE 7. Cumulative plot on log–normal probability paper of the size distribution of droplets shown in figure 6.

50 μm in diameter (as a jet thickens it ejects larger droplets) then about 40 droplets less than 50 μm in diameter will be ejected in a splash. These small droplets are unlikely to disturb the log–normal distribution noted above but they will lower the median size of the droplets below that indicated in figures 6 and 7.

(*c*) *Splashing on thin layers of water*

High-speed photographs were also taken of water drops splashing into layers of water about 0.5 mm in depth. Figure 8, plate 14, shows the main features associated with splashing into such thin liquid layers. There is little difference between the splash produced under these conditions and that produced by a drop impacting on a solid surface. In both cases a crown is formed, jets develop on the periphery of the crown, and the jets become unstable and break up

into fragments. However, the time-scale of the events associated with splashing on a solid surface is much shorter than for splashing into shallow liquids. For example, whereas the crown collapses in about 1.6 ms after impact for splashing on a solid surface, for the same size drop and impact speed it takes more than fives times longer to collapse when splashing occurs on a shallow liquid. The reason for this is that once the crown forms the smoother the surface on which it rides the longer it persists. Figure 9 shows the diameter of the base of the crown and its radial velocity as a function of time for splashing on shallow water and on a solid surface. It can be seen that the radial velocity of the base of the crown is similar for these two cases. Hence,

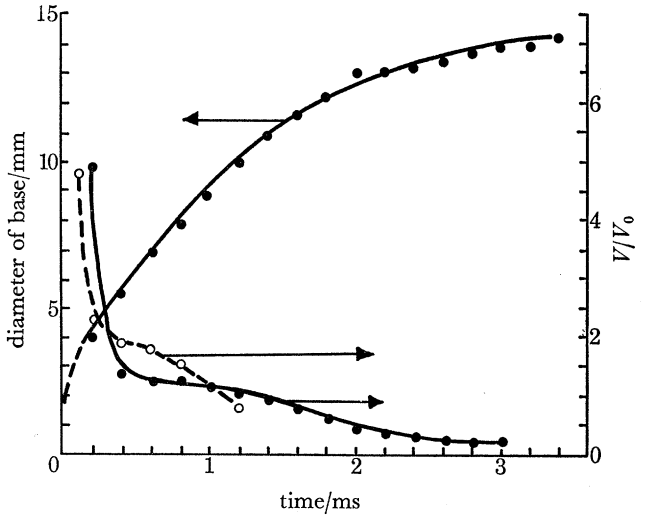

FIGURE 9. Diameter of the base of the crown as a function of time measured from the moment of impact for splashing onto (●) a layer of liquid 0.5 mm in depth and (○) splashing onto a solid surface. Also shown is the ratio of the radial speed V of the crown base to the impact speed V_0. The impact speed in both cases was 4.8 m s^{-1}.

the presence of a thin layer of water does not help in the conversion of the kinetic energy of the drop to the kinetic energy of motion of the base of the crown. The height of the crown wall formed by splashing into a shallow liquid is greater than that which results from splashing on a solid surface. This is because in the former case a small cavity is formed beneath the surface of the liquid, and the liquid displaced by this cavity is incorporated into the wall of the crown.

In §3 of this paper the electrical charges separated by water drops splashing on melting ice are considered with reference to the electrification of natural clouds. Many photographs were taken of splashing on melting ice, however, there were no detectable differences between these splashes and those produced by water drops splashing into thin layers of water resting on other solid materials.

(*d*) *Formation and break-up of the crown*

We now consider in more detail the mechanism by which the crown is formed during splashing.

When a cylindrical jet of liquid impacts on a solid surface the liquid flows radially outward from the jet over the solid surface (figure 10*a*). This flow continues as long as the pressure-head from the vertical jet is maintained. Water droplets may be shed from the perimeter of the liquid sheet which spreads over the solid surface but a crown does not form. When a drop

impacts on a rough solid surface the fluid moves both radially outward over the surface and also upward to form the crown. In fact, a small crown is formed even before appreciable radial motion ensues. To explain the differences between the splashing of a jet and a drop it is necessary to consider in more detail the region near the solid surface at the moment of impact of a drop.

When a drop impacts on a solid surface a shock front is formed which moves outward from the initial point of contact into the collapsing drop. Hence, portions of the drop which are moving downward are diverted radially outward (i.e. parallel to the solid surface) by the advancing shock front. Once some radial motion has been established a narrow neck with a very high convex curvature will be formed (figure 10*b*) and in this region the resultant of the surface tension forces is directed at an angle to the horizontal. If the solid surface is very smooth the

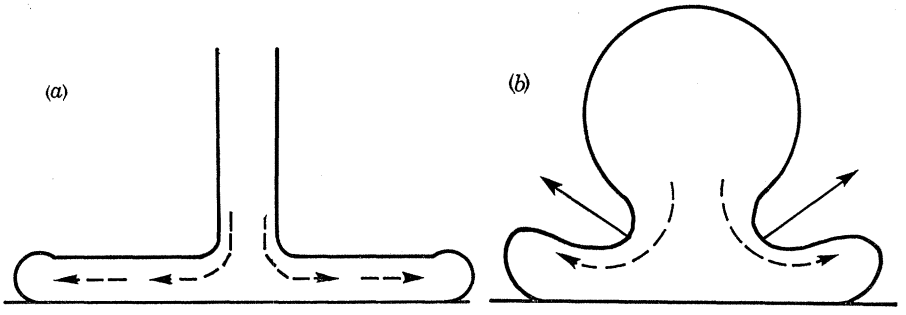

FIGURE 10. Schematic diagram of (*a*) radial flow due to impact of a jet of liquid on a solid surface and (*b*) flow due to impact of a drop on a solid surface (full arrows indicate resultant forces due to surface tension at the neck of the drop).

initial energy can easily be converted into a radial flow on the surface and in this case a crown fails to form. However, on a rough surface the energy conversion into the radial flow is not as efficient and the upward component of the surface tension at the neck and the excess pressure in the drop force the fluid radially outward over the surface but with an upward velocity component. Similar effects of curvature and excess pressure occur in the coalescence of two drops (Bowden 1966).

The outward movement of the fluid across the solid surface creates vorticity the vector of which is parallel to the solid surface. This vorticity is undoubtedly one of the driving forces in the creation of the crown. However, a similar vorticity is present when a jet of liquid collides with a solid surface but a crown is not formed in this case, hence this vorticity alone is apparently not sufficient to create the crown.

We have seen that a rough surface is conducive to the formation of a crown during splashing but irregularities on the surface of the target also initiate disturbancies in the fluid which grow rapidly and cause the crown to break up in a shorter time than for splashing on a liquid surface. More detailed inspection of the crown (figure 11, plate 15) reveals that these disturbances are in the form of waves on the wall of the crown. Taylor (1959*a*) has discussed the development of similar waves on the surfaces of thin sheets of liquid. He observed that these capillary waves could generally be classified into two groups: symmetrical and antisymmetrical. In the symmetrical waves the displacements of the walls of the sheet are in opposite phase and in the antisymmetrical waves they are in phase. During the propagation of symmetrical waves the thickness of the liquid varies so they can be observed in transmitted light. Since the thickness of the liquid does not vary during the propagation of antisymmetrical waves they are best viewed

PHILOSOPHICAL TRANSACTIONS OF THE ROYAL SOCIETY A MATHEMATICAL, PHYSICAL & ENGINEERING SCIENCES

in reflected light. The photograph shown in figure 11 was taken with transmitted light which indicates that the waves are symmetrical. Since high-speed photographs in reflected light could not be obtained, the presence of antisymmetrical waves cannot be ruled out. However, Taylor (1959*b*) observed that symmetrical waves dominate in liquid cones from a swirl atomizer; these cones look very similar to the crowns discussed here. It is reasonable to assume therefore that symmetrical waves dominate on the wall of the crown produced by splashing.

As the crown increases in size a thick cylinder of liquid forms along its upper perimeter which eventually becomes unstable and breaks up into jets. The following argument indicates the manner in which the jets may form. In addition to the symmetrical waves which form parallel to the base of the crown, other waves probably propagate perpendicular to the base of the crown. In fact, streaks could often be seen extending from the solid surface to the top of the crown. In this case, a two-dimensional mesh of waves results which produces variations in the thickness of the crests of the symetrical waves parallel to the base of the crown. As fluid flows into the wall of the crown and is incorporated into the thicker portions of the waves, even larger bulges will form on the top of the crown wall and these may develop into jets. Considerations of the energies involved also reveal a preference for the formation of jets since the surface area of the jets is less than the surface area of the same volume of liquid in the wall of the crown.

The criterion for the break-up of the jets into fragments is not identical to that given by Rayleigh (1879) because the jets which form on the crown are turbulent and the fragments which are thrown off are not spherical. However, to a first approximation, Rayleigh's criterion probably applies to the jets which form on the crown.

Observations of the crowns which form when water drops splash on rough solid surfaces have revealed their similarity to 'water bells'. A 'water bell' is formed when a laminar jet of liquid impinges on a small conical-shaped object. Taylor (1959*c*) derived the following equation for the meridional cross-section of a 'water bell':

$$X = \cos\theta[\cosh^{-1}(\sec\theta) - \cosh^{-1}\{(1-Y)\sec\theta\}], \tag{1}$$

where θ is the initial half-angle of the water bell and X and Y are non-dimensional coordinates which are related to the dimensional coordinates by

$$\frac{X}{x} = \frac{Y}{y} = \frac{4\pi\sigma_a}{\rho Q u_0}, \tag{2}$$

where, σ_a is the surface energy of the liquid–air interface, ρ the density of the liquid, Q the rate of flow of liquid in the jet, and u_0 the velocity of the jet.

Figure 12, plate 15, is a composite photograph obtained by superimposing successive high-speed photographs of the growth of the crown produced by a splash so that the base of the crown in any one frame was made coincident with the upper part of the crown in the preceding frame. The appearance of the crown in this photograph is very similar to a 'water bell'.

The initial half-angle of the crown shown in figure 12 is found by extrapolation to be about 60°. From the total time for disappearance of the drop ($\Delta t = 1.5$ ms), the total volume of the drop ($V = 13 \times 10^{-3}$ cm^3), and the growth velocity of the crown, the values of Q and u_0 were found to be 8.5 cm^3 s^{-1} and 77 cm s^{-1}, respectively. The shape of the 'water bell' obtained by substituting these values into equation (1) is shown in figure 13 where it is compared with measurements on the crown which have been taken from the photograph shown in figure 12. The similarity between the two curves is striking. They begin to deviate significantly when

x exceeds 3 mm which is the point at which the crown becomes unstable and large jets form on its upper periphery. This analogy between the crown formed by splashing and the 'water bell' aids our understauding of the mechanism involved in the formation of the crown.

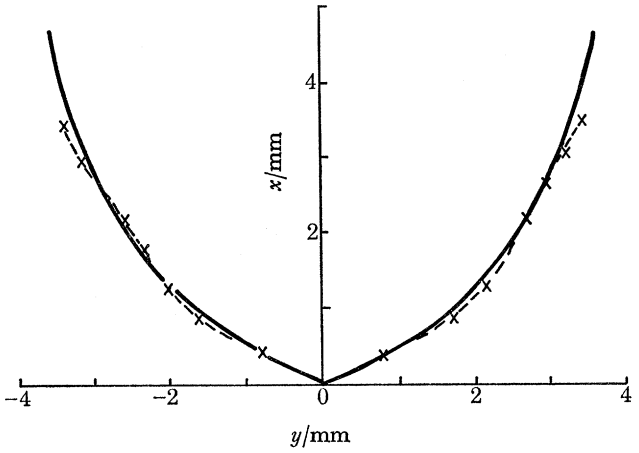

FIGURE 13. Comparison of (× - - ×) the observed shape of a crown with (——) the theoretical curve for a 'water bell'.

3. THE CHARGE SEPARATION

3.1. *Review of previous work*

Interest in the electrical charges separated by the splashing of water drops started with the work of Lenard (1892), who observed that there was a negative space charge in the air in the vicinity of waterfalls. In laboratory experiments he was able to produce similar space charges by splashing water drops onto solid surfaces covered with water. Lenard suggested that the small fragments of water produced in a splash carry negative charges while the large fragments carry positive charges. Thompson (1894) carried out similar experiments using different target materials covered with water. He found that the charging was independent of the nature of the material on which the water rested but it varied with the impurities in the drop and the nature of the gaseous environment. In a later paper Lenard (1915) suggested that negative and positive layers of charge (now known as the 'electrical double layer') are present near the water–air interface and that when a mass of water breaks up charges are separated as a result of the disruption of this layer. Lenard estimated that about 2 pC of charge are separated for each square centimetre of new water surface created by a splash. Nolan & Enright (1922) found that charges of the order 0.60 pC cm^{-2} can be separated when water is broken up by air currents.

The concept of the electrical double layer has been developed theoretically by Gouy (1910) and it has received support from experimental work on the motion and the bursting of bubbles in liquids (Coehn & Mozer 1914; Alty 1924, 1926; Bach & Gilman 1938; Blanchard 1963; Irbarne & Mason 1967), the atomization of liquids (Frumkin & Obrutschewa 1931; Chapman 1938*a*, *b*) and the break-up of liquid jets (Jonas & Mason 1968). According to present ideas this layer is composed of a compact region of negative charges at the surface of the water–air interface and a diffuse region of positive charges at the surface of the water–air interface and a diffuse region of positive charges immediately below the negative charges. About one in every thirty molecules is oriented normal to the water–air interface and the potential difference across the interface is about 0.26 V.

It is believed that the diffuse layer can move past the compact layer under the action of suitable forces. The current that results from such a mechanism is called the 'streaming current'. We have shown in §2 that the jets which form on the crown produced by a splash develop instabilities which grow and finally result in the break-up of the jet. As the disturbances grow on the jet, liquid is forced outwards from the narrow necks past the compact layer. As a neck decreases in radius a point is reached, just before break-up, when it contains only the negative charges of the compact layer. Jonas (1968) has shown that the total charge separated by the streaming current depends on the size of the fragments which break away from the jet. For the large jets the streaming current can carry a positive charge of about 3 fC provided that the concentration of impurity in liquid is greater than about 10^{-4} mol l^{-1}. The charge is reduced for lower concentrations of impurity and for smaller jets. If the liquid is conducting, reverse bulk and surface currents will be established and these will reduce the maximum possible charge which can be separated by the streaming current.

In addition to the disruption of the electrical double layer, several other mechanisms can contribute to the separation of charges when liquids break up. For example, in the bulk of a liquid the ions are distributed at random and when the liquid is disrupted any one fragment may carry quite a large net charge of either sign. However, the charges on the fragments produced by this mechanism will be statistically distributed and the mean charge should be close to zero. If a liquid is in contact with another material the charges produced when the liquid is broken up may be affected by the contact potential between the liquid and the material. However, contact potentials are relatively small and under normal circumstances probably do not contribute greatly to the charging. When liquids break up in the presence of electric fields the fragments which are produced may carry appreciable charges of one sign due to polarization effects (so called 'induction charging'). Finally, in the particular case of water drops splashing on ice, which will receive some attention in this paper, the possible effects of freezing on the charge separation must be considered. Workman & Reynolds (1950) have shown that potential differences of the order several hundred volts can develop across the ice–water interface during the freezing of aqueous solutions. Ice also exhibits a thermoelectric effect (Latham & Mason 1961) which might affect the charges separated in a splash.

The role of the above mechanisms in separating charges during splashing under various conditions are considered in relation to the experimental observations in §3.3.

3.2 *Experimental*

The purity of the water drops was a critical factor in obtaining consistent experimental results on the charges separated by splashes. In order to prevent contamination of the water drops by impurities in the air, a system was constructed so that the water did not come into contact with air after it had been purified. A schematic of the purification system is shown in figure 14. The water was initially distilled in an all-glass vessel, after which it was passed through two ion-exchange columns. The water then passed into vessel C, which was flushed with nitrogen, and after further distillation was collected in reservoir A. If pure water was desired, the water from A was then transferred via a conductivity cell into vessel D from which it was fed into the drop generator. However, when known concentrations of impurity were needed in the water, a measured amount of solute was placed in vessel B and mixed in a nitrogen atmosphere with a measured quantity of water from A. The solution was then transferred via the conductivity cell to vessel D and the drop generator.

PHILOSOPHICAL TRANSACTIONS OF THE ROYAL SOCIETY A MATHEMATICAL, PHYSICAL & ENGINEERING SCIENCES

The apparatus in which the splashing took place (figure 15) was constructed solely of glass, stainless steel and polyethylene and it was filled with nitrogen gas. Water drops from the drop generator fell through the Pyrex tubes and as they entered the cylindrical stainless steel case they

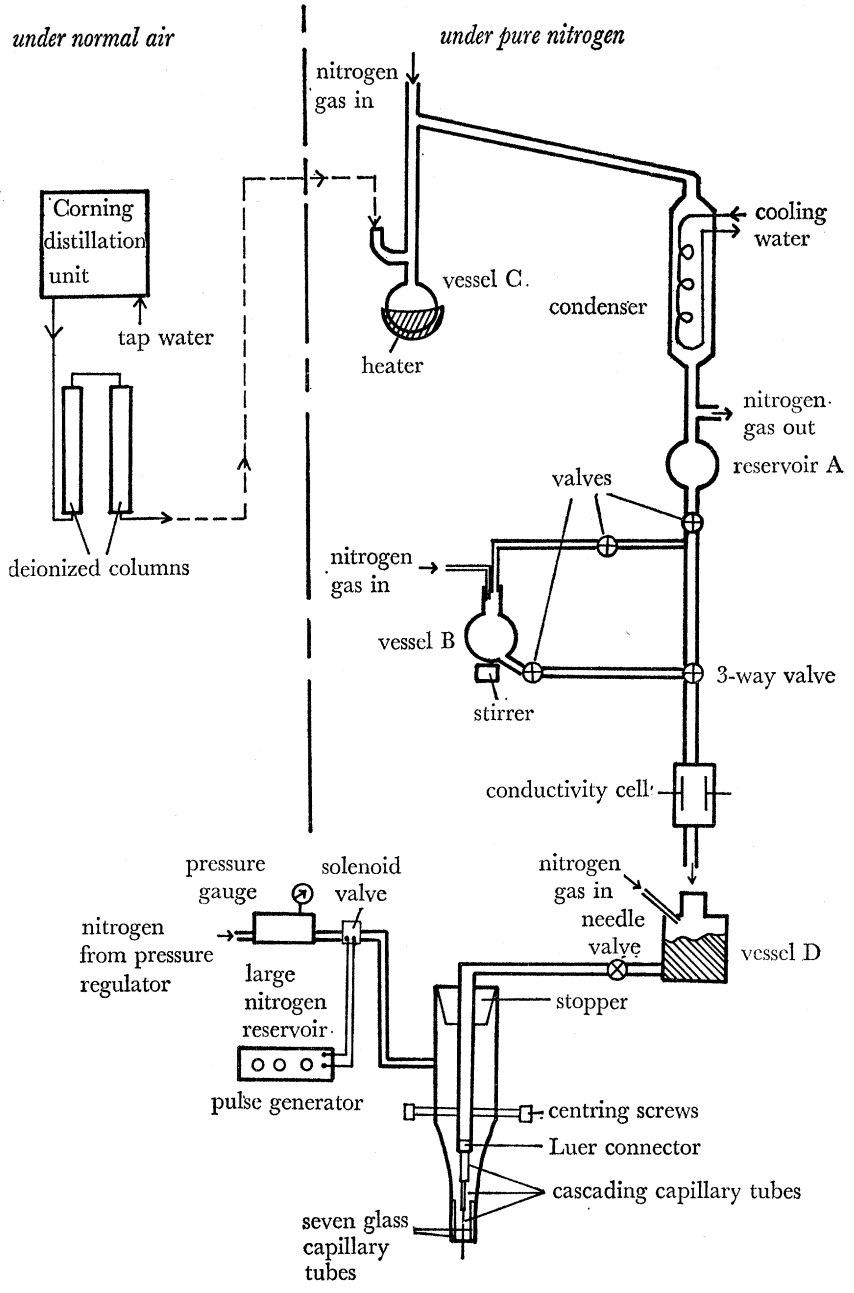

FIGURE 14. Schematic diagram of the apparatus for purifying the water and the drop generator.

passed through an induction ring (4.8 cm in diameter and 2.4 cm high) connected to an electrometer which we will refer to as the 'ring electrometer'. This electrometer was similar to the one described by Scott & Levin (1970); the circuit diagram is shown in figure 16. If the drops were charged they generated a pulse in the ring electrometer which was recorded on a

fast response oscillograph. These pulses were proportional to the charge on the drops. The charge on the falling drops could be controlled by applying a potential between the drop generator and ground. A negative potential of about 0.900 V had to be applied to the needle in order to reduce the charge on the drops to zero.

After passing through a grounded shield, the drops entered a region between two parallel plates where controlled vertical potential gradients could be applied. The drops then collided

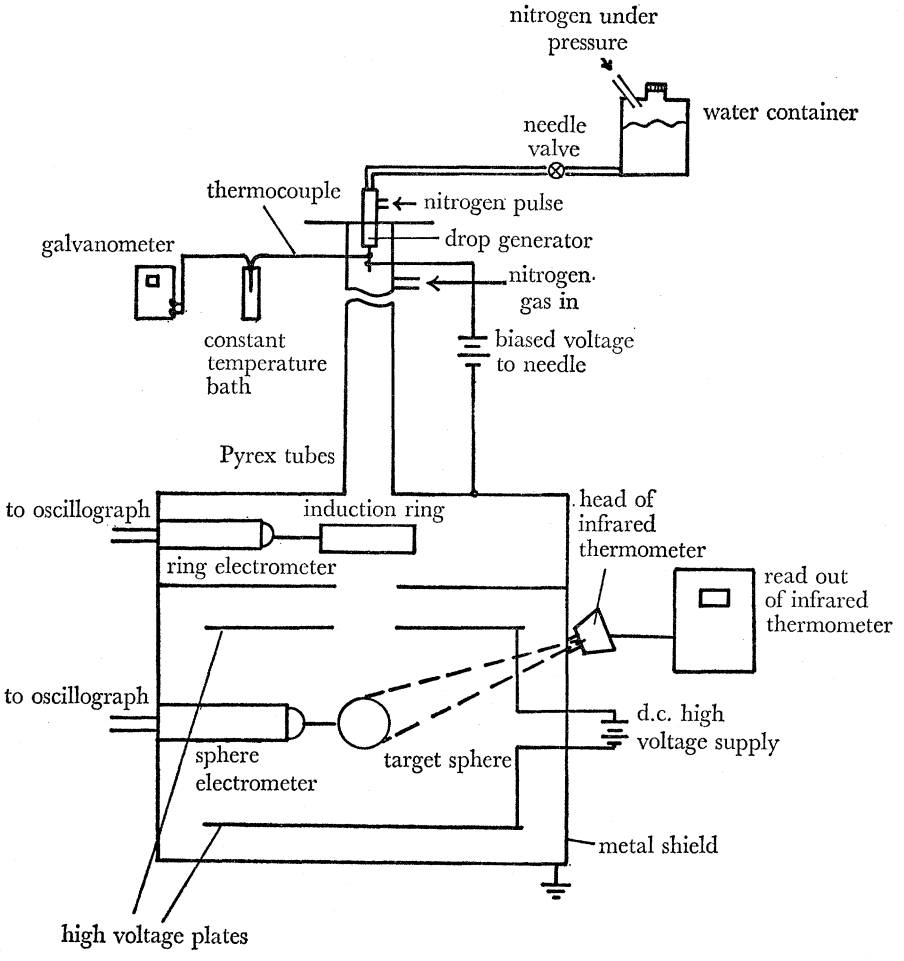

FIGURE 15. Schematic diagram of the splashing apparatus.

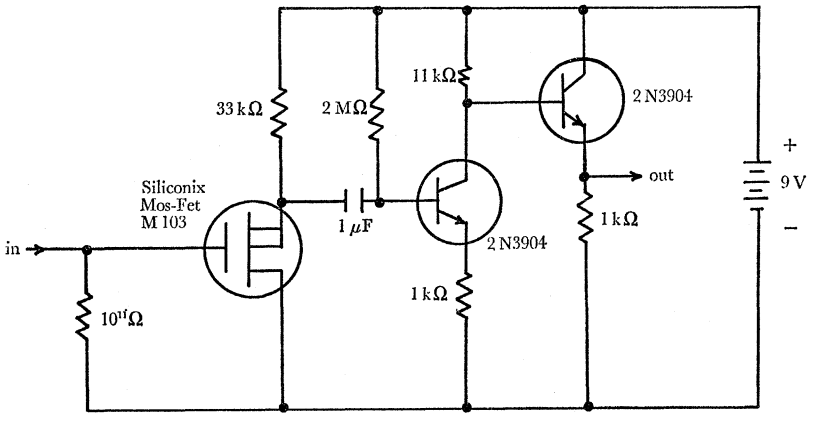

FIGURE 16. Circuit diagram of the ring and sphere electrometers.

11

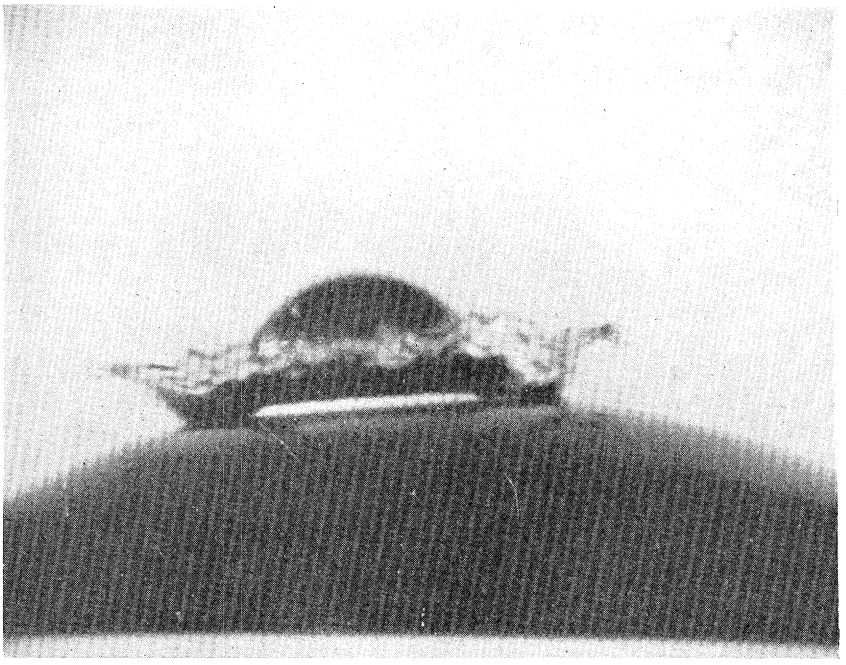

12

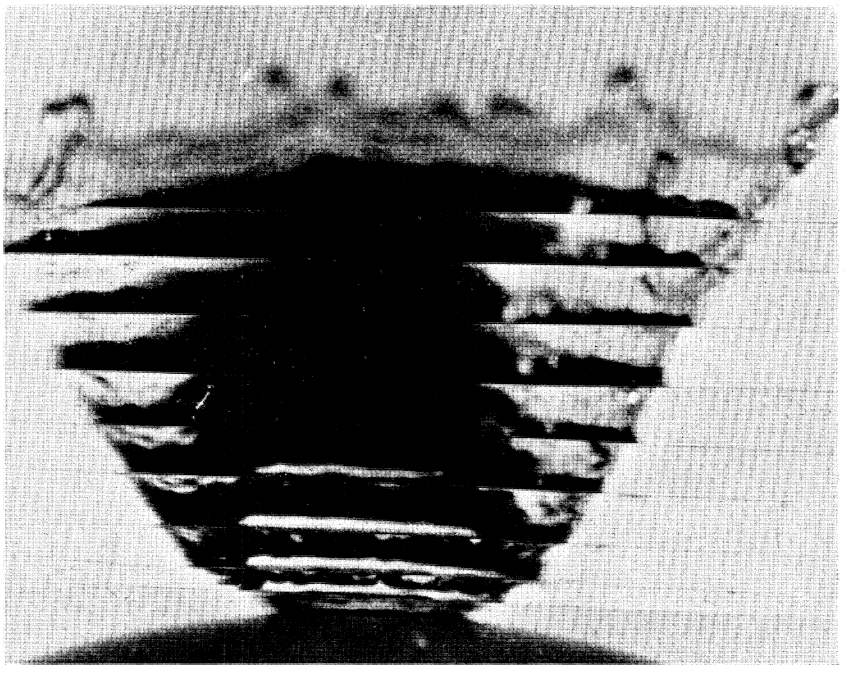

FIGURE 11. Symmetrical waves on the wall of the crown viewed with transmitted light. (Magn. × 11.5.)

FIGURE 12. Composite photograph illustrating the growth of the crown.

(*Facing p.* 568)

PHILOSOPHICAL TRANSACTIONS OF THE ROYAL SOCIETY A MATHEMATICAL, PHYSICAL & ENGINEERING SCIENCES

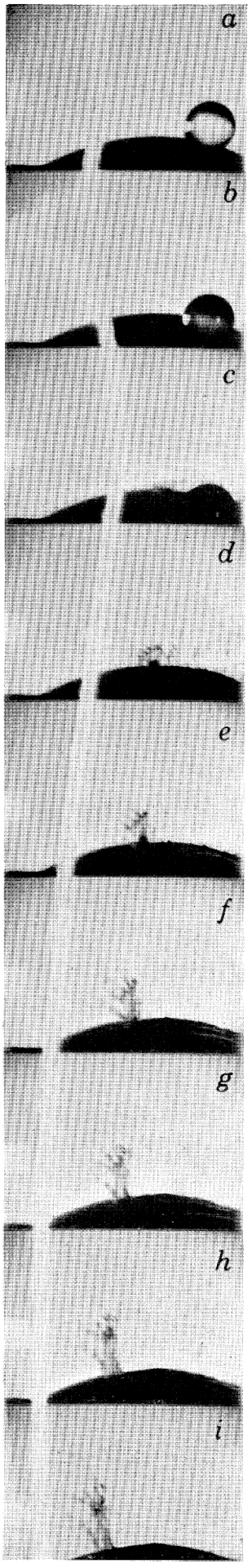

17

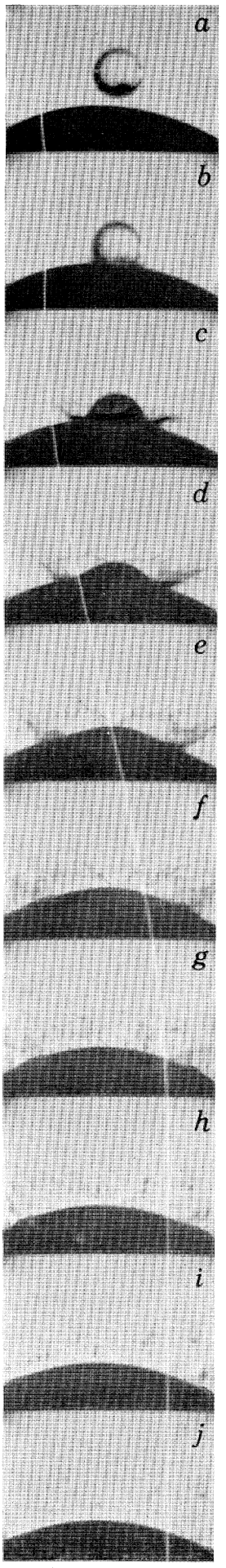

19

FIGURES 17 and 19. For legends see facing page

PHILOSOPHICAL TRANSACTIONS OF THE ROYAL SOCIETY A MATHEMATICAL, PHYSICAL & ENGINEERING SCIENCES

with a sphere (copper or ice) 2.5 cm in diameter which was placed midway between the two parallel plates. The sphere was connected to an electrometer (called the 'sphere electrometer') which had the same type of circuit as the ring electrometer. The electronics of the ring and sphere electrometers were shielded for the prevention of magnetic and electric noise, and they were rigidly mounted in a solid sheath of fused quartz. This arrangement, together with the outside metal shield around the splashing apparatus and the use of batteries throughout the system, resulted in high signal to noise ratios. Both electrometers could detect charges down to 0.3 fC.

The electrical pulses produced by the splash of a water drop on the sphere appeared on the oscillograph as an abrupt transfer of charge followed by a slow bleed-off of this charge through the 10^{11} Ω resistor (figure 16). The charge Q transferred to the sphere was determined from the relation $Q = CV$ where, C is the effective capacity of the sphere electrometer and V the peak value of the voltage output from this electrometer. The capacity C was measured by noting the attenuation of a 1000 Hz signal when a precision 2.2 pF capacitor was placed in series with the input to the sphere electrometer. The value of C was 4.7 pF. The signal output from the ring electrometer was calibrated relative to the sphere electrometer in the following way. The metal sphere was replaced by a wooden cup filled with steel wool and the capacitance of the sphere electrometer was remeasured. The signals from the ring and sphere electrometers were then recorded as water drops carrying various charges passed through the ring and were caught in the wooden cup. Measurements of the heights of the pulses from the ring electrometer showed that its effective capacitance was 6.2 pF.

In some experiments to be described below a signal representing the voltage output from the sphere electrometer was superimposed on high-speed photographs of the splash. This was accomplished by connecting the electrometer to an oscilloscope situated behind the camera and projecting the image of the oscilloscope trace onto the back side of the film strip on the front of which the image of the splash itself was recorded. To obtain a good recording of the oscilloscope trace it was necessary to replace the ordinary cathode-ray tube (P-2) by a higher intensity tube with a fast decaying phosphor. A P-11 tube was found to be very suitable since its colour spectrum peaks near the blue and matched the peak in the colour spectrum of the film (Kodak 4 × N) which was used. Before each experimental measurement a square wave signal generator was used to calibrate the photographic image of the oscilloscope trace.

The equipotential lines between the two parallel plates were not horizontal over the whole volume between the plates because of the hole in the upper plate and the presence of the sphere (figure 15). The equipotential surfaces, in two-dimensions, were determined by drawing the apparatus on graphite paper with high conductivity silver paint. A potential difference was then applied between the two simulated plates and the equipotential surfaces were traced using a galvanometer. These measurements demonstrated that in the vicinity of the sphere the equipotential lines were uniform and parallel.

Description of plate 16

Figure 17. Superimposed photographs of the splashing of a water drop 2.9 mm in diameter on a melting sphere of ice and the signal representing the charges received by the sphere in the absence of an applied electric field. Time interval between frames is 0.2 ms. (Magn. × 2.7.)

Figure 19. Superimposed photographs of the splashing of a water drop 2.9 mm in diameter on a copper sphere and the signal representing the charges received by the sphere in the presence of an applied electric field of -1 kV m^{-1}. Time interval between frames is 0.2 ms. (Magn. × 2.6.)

PHILOSOPHICAL TRANSACTIONS OF THE ROYAL SOCIETY A MATHEMATICAL, PHYSICAL & ENGINEERING SCIENCES

The entire apparatus was either located in a laboratory with a high ceiling, to allow the distance of fall of the water drops to be varied, or in a cold room to permit measurements at different temperatures. The temperature of the ambient gas was recorded throughout an experiment. In addition, a thermocouple was connected to the needle of the drop generator for measurements of the temperatures of the water drops at the moment of their release. The temperature of the surface of the sphere could not be measured directly with a thermocouple since this would have interfered with the charge measurements. However, this temperature was measured approximately by pointing a Barnes infrared thermometer at it through a special opening in the cylindrical case (figure 15).

The sequence of steps associated with a normal experimental measurement was as follows. The splashing apparatus was flushed with dry nitrogen gas for about 10 min before an experiment. The water (or solution) sample was connected to the drop generator which was adjusted to produce about one drop per second. The copper sphere, which between experiments was stored in a dichloroethane solution, was carefully washed in deionized water and then mounted in the apparatus. Ice spheres were prepared by filling hollow glass balls with deionized water and placing them in a cold box. When the water had frozen the glass shells were broken off and the surfaces of the ice washed with deionized water. To prevent contamination the metal and ice spheres were handled with clean dry forceps. Since we were generally interested in measuring only the charges produced by splashing, any initial charges on the drop were eliminated by varying the bias voltage to the needle of the drop generator until the falling drops produced zero output from the ring electrometer. The speeds of impact of the drop with the sphere were measured by noting the time interval between the signals from the ring and sphere electrometers.

3.3. *Results and discussion*

(*a*) *Relation between the splash and charge separation*

Superimposed high-speed photographs of a splash and the electrical signals representing the charges produced by the splash revealed the relation between the charge separation and the details of the splashing event. Figure 17, plate 16, shows a sequence of such photographs in the case of a water drop 2.9 mm in diameter splashing onto a melting sphere of ice with an impact speed of 4.8 m s^{-1}. After leaving the drop generator the drop carried a positive charge of about 3.3 fC. The surface temperature of the ice was close to 0 °C and the thickness of the liquid layer was not more than 0.25 mm. There was no applied electricfield. The electrical signal generated by the splash is indicated by the broad white line on the photographs. A deflexion of this line to the left indicates that the sphere is becoming positively charged and a deflexion to the right that is becoming negatively charged. Similar signals to those shown in figure 17 were generated by splashing onto metal surfaces.

On (or just before) collision, the electrical signal rises quickly (figure 17*b*). This is due to the charge carried on the drop; in the case of uncharged drops this initial fast-rising signal is not seen. Most of the photographs showed a double hump on this initial signal, the first occurring at about 10 μs and the second at about 30 μs from the time at which the signal first began to rise. The first hump may be due to the transfer of charge to the sphere through the air before the drop actually makes contact with the sphere. Atkinson & Paluch (1966) have shown experimentally that electric sparks can jump between two charged drops separated by a small distance. The second hump would then represent the charge transferred when the drop collided with the sphere. This explanation is reasonable since as soon as conduction begins between the

sphere and the approaching drop the electric field between them would decrease and quickly fall below that required to continue the discharge. Hence, it is unlikely that the drop would lose all of its charge due to the discharge. After impact, the initial rising signal quickly decays to a small, but not zero, value within about 200 μs (figure 17*b*, *c*). This is probably due to the deformation of the drop which causes an increase in the mutual capacitance between the drop and the sphere and therefore a decrease in the measured potential resulting from the charge communicated to the sphere.

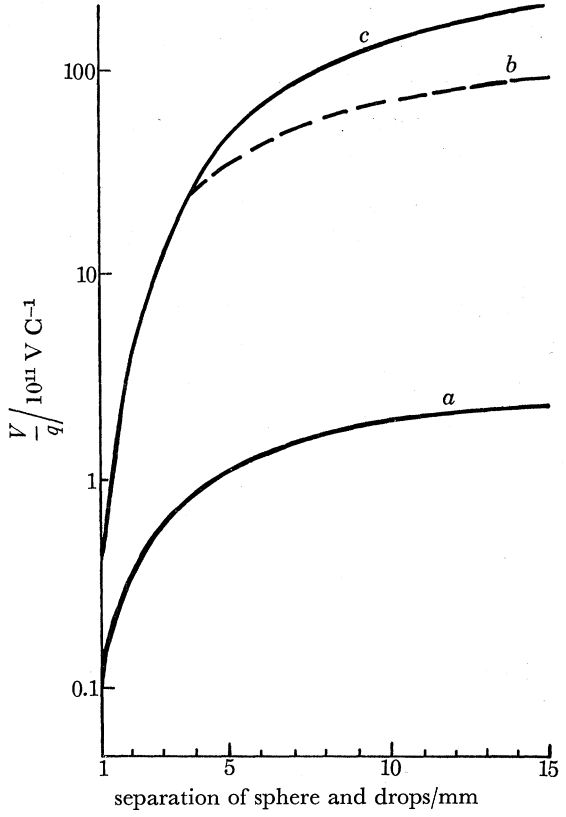

FIGURE 18. Variations in the ratio of the potential V of the sphere to the charge q on the sphere produced by the ejection of charged droplets as a function of the distance between the sphere and the first droplet ejected for: (*a*) one droplet 100 μm diameter, (*b*) 40 droplets 100 μm diameter separated by 50 μm, (*c*) 90 droplets 100 μm diameter separated by 50 μm.

Following the decay of the initial signal, a slower rising signal starts at the same time as fragments begin to be ejected from the jets on the crown (figure 17*c*). This signal continues to move to the left (i.e. the sphere is receiving increasing positive charge) as long as fragments are being ejected from the crown. When no more fragments are ejected the signal returns to zero within a time interval corresponding to the time constant of the sphere electrometer (0.5 s). The rise time of the slower rising signal is about 1.7 ms for splashing into thin layers of water and 1.2 ms for splashing on solid surfaces. These times correspond closely to the time interval between the breakup of the first jet and that of the last jet (hereafter referred to as the total contact time of the jet and the fragment).

If it is assumed that m small non-conducting droplets of equal size, each carrying a charge q/m, are ejected from the crown and that the distance between the individual droplets is large

enough that their mutual capacitance may be neglected, it may be shown that the net charge q left on the sphere due to the ejection of the droplets is given by

$$q = V\left[\frac{C_{33}(C_{11}+C_{22}+2C_{12})-mC_0^2}{C_0+C_{33}}\right]+\frac{Q}{C_{33}/C_0+1}, \tag{3}$$

where V is the potential of the sphere, C_{12} is the mutual capacitance between the electrometer and the sphere, C_{11}, C_{22} and C_{33} are the capacitances of the electrometer, the sphere and the water drop respectively, C_0, the mutual capacitance between each droplet and the sphere, and Q the initial charge on the sphere. Values of V/q as a function of the distance between the sphere and the first droplet ejected from the crown calculated from equation (3) are shown in figure 18. It has been assumed that each of the droplets is 100 μm in diameter and that they are ejected one at a time so that they are separated by a distance of 50 μm. The values of Q has been taken as zero. Curve (*a*), (*b*) and (*c*) are for $m = 1$, $m = 40$ and $m = 90$ respectively. The curves resemble closely the slower rising electrical signal in figure 17 and they provide confirmation that the charging which produces this signal is a result of the ejection of charged droplets from the crown.

Since the time constant of the sphere electrometer was about 100 times greater than the time taken for the droplets to escape from the crown, the peak output voltage V_m from the sphere electrometer corresponds to the potential of the sphere when the droplets are far removed from it. Hence, the total charge q separated by the splash can be found from the relation

$$q = V_m C_m, \tag{4}$$

where, C_m is the effective capacitance of the sphere and electrometer system.

Superimposed photographs of a splash and the electrical signal representing the charges produced by the splash in the case when a vertical electric field of -1.0 kV m^{-1} (minus sign indicates that the potential of the upper plate was negative with respect to the lower plate) was applied are shown in figure 19, plate 16. The water drop was 2.9 mm in diameter and it splashed onto a copper sphere after falling through a distance of 145 cm. After leaving the drop generator the drop carried a negative charge of about 3.3 fC. A fast rising electrical signal (figure 19*b*) moving to the right is seen on these photographs at, or just before, impact. A double hump on this portion of the signal is not discernible but this is simply due to the fact that the gain of the amplifier on the oscilloscope was set at a comparatively low value. Following the initial signal a slower rising signal, also moving to the right, appears at the same time as fragments are ejected from the jets of the crown. The charge received by the copper sphere due to the ejection of fragments from the crown was one hundred times greater in this case than that shown in figure 17, and the sphere received a negative rather than a positive charge. These results demonstrate the effectiveness of applied electric fields in determining both the magnitude and the sign of the charge separated by splashing.

In the measurements described below, unless it is stated otherwise, the drops were initially uncharged and an electric field was not applied.

(*b*) *Effects of impurities*

The mean charges separated by drops, 2.5 mm in diameter, containing various concentrations of sodium chloride after impacting with copper and ice spheres with a velocity of 4.1 m s^{-1} are shown in figure 20. The measurements were made at 0 °C. The bars on each experimental

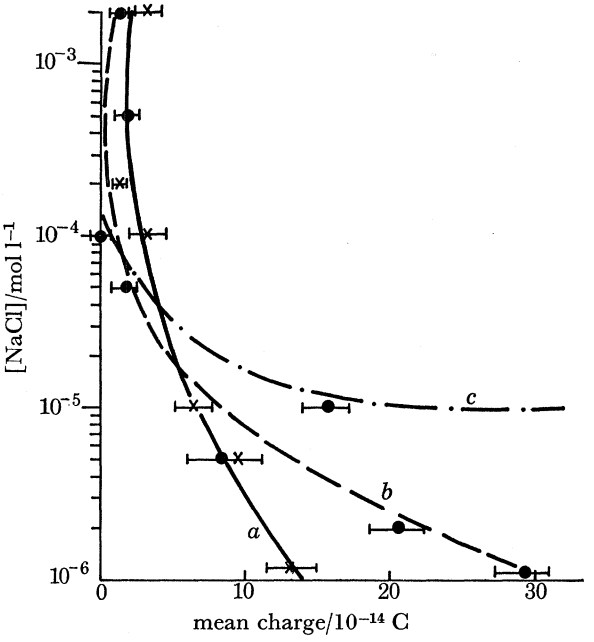

FIGURE 20. Mean charges transferred at 0 °C to: (*a*) a copper sphere, and (*b*) an ice sphere by the splashing of drops 2.5 mm in diameter containing various concentrations of sodium chloride. Curve (*c*) is based on theory (see text).

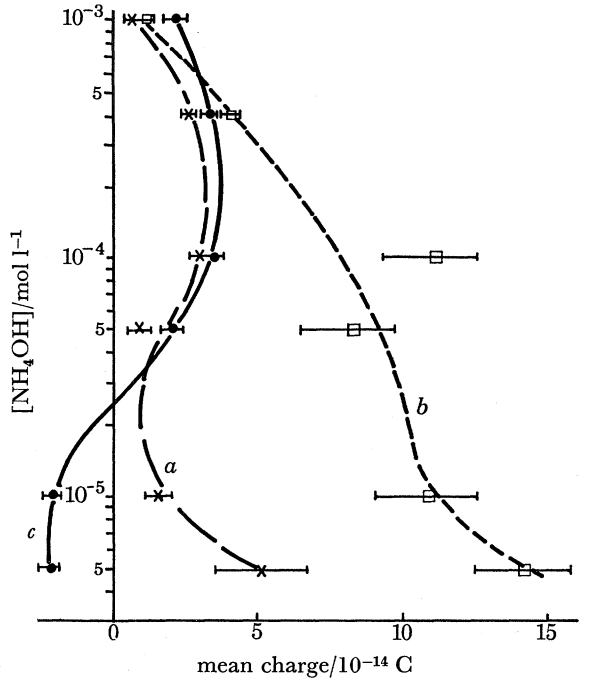

FIGURE 21. Mean charges transferred to (*a*) an ice sphere at +1 °C, (*b*) a copper sphere at 0 °C, and (*c*) an ice sphere at −1 °C by drops 2.5 mm in diameter containing various concentrations of ammonium hydroxide which impacted on the surfaces with a speed of 4.1 m s^{-1}.

point represent the maximum error in measuring the individual charges. It can be seen from the two experimental curves (*a* and *b*) that the magnitude of the charges separated increases with decreasing concentration of ions in the solution. The spheres were generally left with a positive charge so that the liquid fragments ejected in the splash carried off a net negative charge. For higher concentrations of sodium chloride about the same amount of charge is separated for splashing on copper as on ice. However, for lower concentrations of sodium chloride more charge is separated when splashing occurs on ice than on copper.

The results of experiments carried out at different temperatures for drops containing different concentrations of ammonium hydroxide which splashed onto ice and copper are shown in

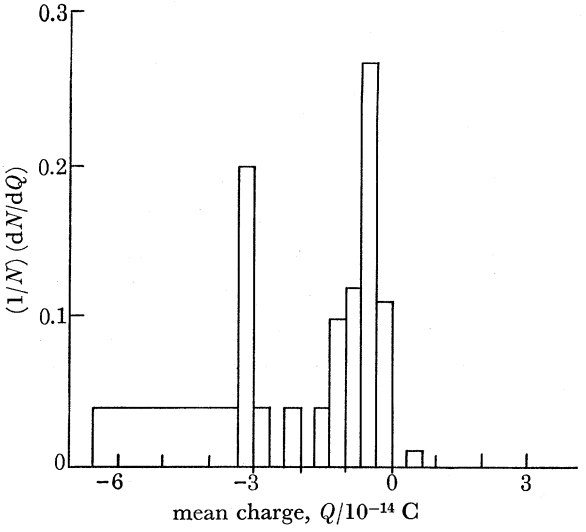

FIGURE 22. Normalized distribution of the charges transferred to an ice sphere at −1 °C due to the splashing of drops containing 5 μmol l^{-1} of ammonium hydroxide solution. The drops were 2.5 mm in diameter and they collided with the sphere with a speed of 4.1 m s^{-1}.

figure 21. For splashing on ice at +1 °C and copper at 0 °C, the positive charges left on the spheres tended to increase in magnitude with decrease in solute concentration. However, for splashing on ice at −1 °C the charges received by the sphere were positive for high concentrations of ammonium hydroxide, reaching a maximum for concentrations of about 10^{-4} mol l^{-1}, but it was negative for low concentrations. In this case the ice increased in thickness by 0.5 mm in about 100 s. These results can be partially explained in the following way. Workman & Reynolds (1950) found that when aqueous solutions of ammonium hydroxide were frozen, high potential differences developed across the ice–water interface due to the preferential incorporation of NH_4^+ ions into the ice lattice. This selective incorporation left the solution with a negative charge. Pruppacher, Steinberger & Wong (1969) found that for spontaneous freezing a maximum potential difference was developed when the concentration of ammonium hydroxide was 10^{-4} mol l^{-1}. Now in the experiments described above a thin layer of solution resided on the ice surface at −1 °C, as this slowly froze the solution would have become negatively charged with respect to the ice. When a solution drop splashed into this layer, fragments from the drop and the layer would be ejected carrying a net negative charge. The ice sphere would then be left with a positive charge, as observed for drops containing more than 2.5×10^{-5} mol l^{-1} of ammonium hydroxide (figure 21, curve *c*). The reason for the reversal of the charging at lower concentrations of ammonium hydroxide in the case of drops at −1 °C splashing onto

ice is not clear. However, it is possible that the thermoelectric effect in ice is beginning to play a role and to charge the ice negatively as observed by Latham & Mason (1961) when supercooled water drops impact on ice.

Figure 22 shows the distribution of charges left on an ice surface at -1 °C due to the splashing of drops containing 5 μmol l^{-1} of ammonium hydroxide solution. This distribution, like many others (see below), was found to be log–normal. The median charge left on the sphere was -0.0133 pC and the geometric standard deviation was 0.31.

It has been shown above that most of the charge separation in splashing results from the ejection of the small fragments (about 10 μm in radius) which are released from the jets during their early stages of growth. When a fragments breaks away from a jet it will tend to carry a net negative charge due to the electric double layer. If it is assumed that the jets are formed from a layer of thickness 0.3 μm near the surface of the crown it may be shown that the total charge Q carried by n fragments (assumed spherical and of radii $r_1\ r_2 \ldots r_n$) due to the effect of the double layer is given by

$$Q = -9.5 \times 10^9 c^{\frac{1}{2}} \exp\left[-\tfrac{1}{2} - 10^3 c^{\frac{1}{2}}\right] \sum_1^n r_n^3, \tag{5}$$

where c is the concentration (mol l^{-1}) of the aqueous solution. A similar equation to (5) was derived by Iribarne & Mason (1967) for the charge released by the bursting of bubbles of air in aqueous solutions. Hence, if the separation of charge which occurs on splashing were due entirely to the disruption of the electric double layer, (5) should give a good approximation to the actual charges observed. The charge separation predicted by this equation for the case when one droplet is ejected from a jet of diameter 20 μm is shown in curve (*c*) in figure 20. The theoretical curve resembles the experimental curves, but the measured charges are obviously much less than those predicted by (5). This discrepancy could be due to the streaming currents which will tend to offset the charging produced by the electrical double layer. However, since the mean charges received by the surface on which the splashing occurred were positive, the charging due to the disruption of the electrical double layer apparently dominates over that due to the streaming current.

It has been shown in §2 that the sizes of the droplets ejected in a splash are log–normally distributed. When a size distribution is log–normal all parameters which depend on the radius raised to some power also follow a log–normal distribution (Herden 1960). Hence, if the charge separation were described by (5) the charges carried on the fragments from a splash would follow a log–normal distribution. Similarly, if we assume that the *mean sizes* of the droplets from splashes follow a log–normal distribution, then the mean charges received by a surface due to the splashing of drops would be log–normally distributed as found experimentally.

(*c*) *Effects of impact speed and size of drop*

The average charges separated by the splashing of water drops 2.5 mm in diameter on a copper sphere at various impact speeds are shown in figure 23. Curve (*a*) is for drops consisting of dilute solutions of sodium chloride (2×10^{-4} mol l^{-1} and conductivity 2.8 mS m^{-1}), and curve (*b*) is for doubly distilled water (conductivity 16 μS m^{-1}). It can be seen that the charges separated by splashing increase with increasing speed of impact. It should be noted that the terminal speed for a drop 2.5 mm in diameter falling through air is about 6.5 m s^{-1}.

These results support the conclusion that the charge separated during a splash is caused by the ejection of the fragments from the crown. As the speed of impact is increased the number of

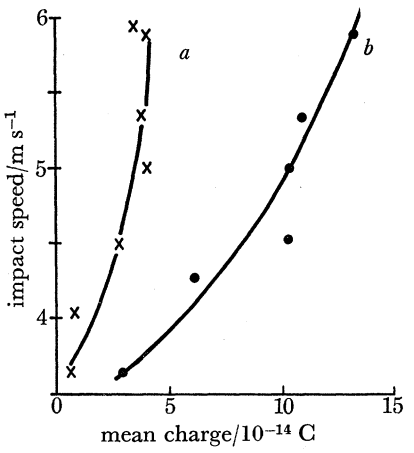

FIGURE 23. Mean charges transferred to a copper sphere as a function of the impact speed of drops 2.5 mm in diameter consisting of (*a*) 2×10^{-4} mol l^{-1} of sodium chloride, and (*b*) pure water. Temperature was 20 °C in both cases.

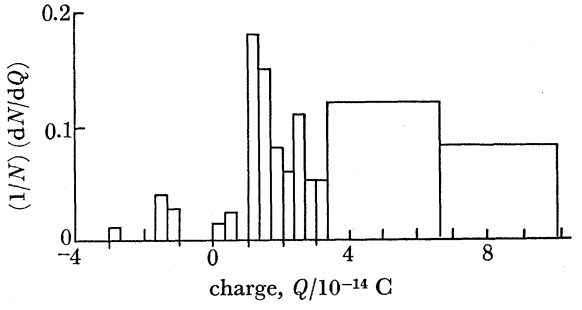

FIGURE 24. Normalized distribution of the charges received by a copper sphere due to the splashing of drops 2.5 mm in diameter and containing 2×10^{-4} mol l^{-1} of sodium chloride which impacted at a speed of 4.5 m s^{-1}. Temperature was 20 °C.

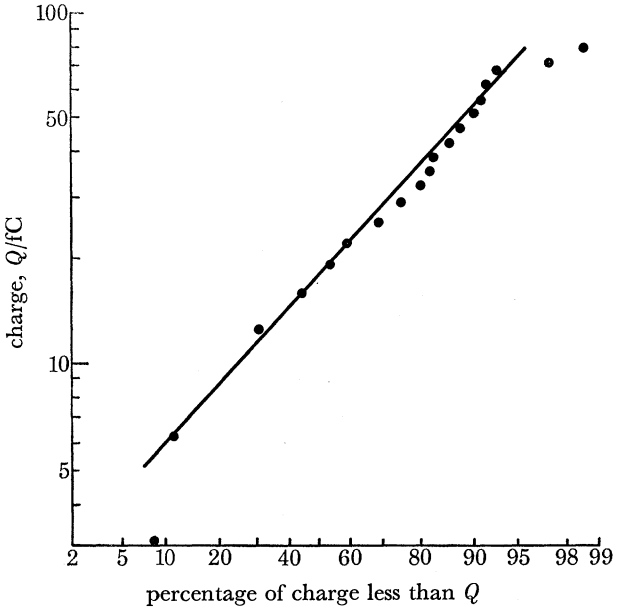

FIGURE 25. Cumulative distribution of the positive charges shown in figure 24 on a log–probability plot.

fragments ejected also increases and hence more charge is separated. However, beyond a certain point a further increase in impact speed does not cause an appreciable increase in the number of fragments but merely increases the speed with which they are ejected. Consequently, the rate of increase in the charge separated is reduced as the impact speed increases above a certain value as seen in figure 23.

The results shown in figure 23 also demonstrate that more charge is separated by the splashing of pure water than by the splashing of dilute solutions of sodium chloride. This result is attributed to the difference in electrical conductivity between the sodium chloride solution and the

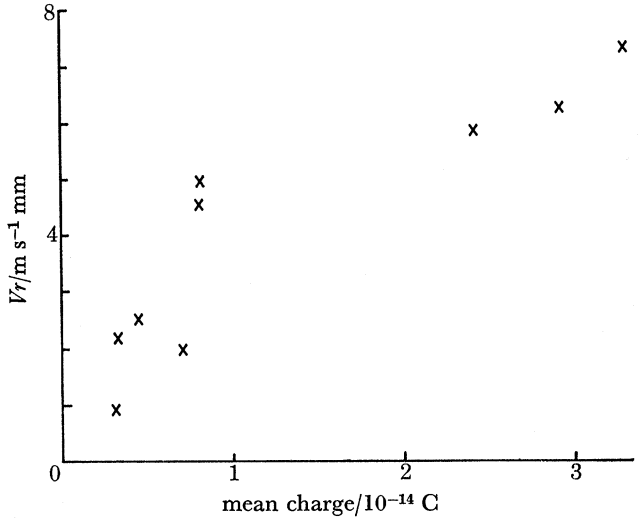

FIGURE 26. Mean charge produced by the splashing of drops on a copper sphere as a function of the product of the speed (V) of impact and radius (r) of the drop.

TABLE 2. SUMMARY OF CHARGES SEPARATED BY DROPS OF DIFFERENT SIZES IMPACTING AT DIFFERENT SPEEDS ONTO A COPPER SPHERE (DROPS CONTAINED 2×10^{-4} mol l^{-1} OF SODIUM CHLORIDE)

radius of drop mm	electrical conductivity/mS m^{-1}	impact speed m s^{-1}	number of events recorded	mean charge transferred to sphere fC	median charge transferred to sphere fC
0.27	2.5 ± 0.2	4.5	94	3.76	0.666
1.25	2.4 ± 0.2	3.65	75	8.57	7.33
0.50	2.4 ± 0.2	4.0	79	7.33	6.66
0.90	2.4 ± 0.2	2.65	104	5.00	6.00
0.75	2.8 ± 0.2	2.88	111	3.83	9.66

pure water. As charge is separated in the jets, reverse currents in the bulk of the liquid will tend to counteract the charging mechanism. Since the total time for a fragment to break away from a jet is small, the higher the electrical conductivity of the bulk liquid the more charge will be carried by the reverse currents and the less charge will be carried away on the fragments.

The results obtained with pure water showed considerable variability and a large number of individual measurements were needed in order to obtain a reliable average value for the charging. This was probably due to the presence of random traces of impurities, which were not removed by the purification system, and to statistical charging.

Figure 24 is a normalized histogram of the charges received by the copper sphere due to the splashing of the sodium chloride solution drops at an impact speed of 4.5 m s^{-1}. Both positive

and negative charges were observed but over 90 % of the charges were positive. The cumulative distribution of the positive charges are plotted in figure 25 on log–probability paper. The experimental points lie approximately on a straight line which indicates that the distribution is log–normal. The median charge 0.019 pC and the geometric standard deviation 2.2.

A series of measurements were made of the charges separated by drops of various sizes splashing onto the copper sphere. The results are summarized in table 2. In figure 26 the mean charges are plotted against the product of the speed of impact V and the radius r of the drop. It can be seen that the mean charge transferred by splashing increases approximately linearly with Vr. Since an increase in either V or r will generally cause an increase in the number of fragments ejected this result is understandable. Rupe (1950) found that water drops splash in paraffin when Vr exceeds 0.94, where r is in mm and V in m s^{-1}. The trend of the data in figure 14 indicates that the cut-off value of Vr for splashing to occur on a metal surface is less than 0.94, however, this can be attributed to the difference in the target surfaces used in the two cases.

(*d*) *Effect of temperature*

The effect of temperature on the charges separated by splashing was investigated by taking measurements at 20, 10, 5 and 0 °C for drops 1.25 mm in radius impacting at a speed of 4.1 m s^{-1} onto a copper sphere. Both dilute solutions of sodium chloride and doubly distilled water were used. A consistent variation of the mean charge separated by splashing with charge in temperature was not observed, although the charge appeared to decrease slightly as the temperature was lowered from 10 to 0 °C.

The parameters involved in charge separation by splashing which vary with temperature are the surface tension of the liquid and its electrical conductivity. As the temperature decreases from 20 to 0 °C, the surface tension increases slightly and the electrical conductivity decreases slightly. An increase in surface tension will tend to reduce the number of fragments ejected in a splash, while a decrease in conductivity will increase the charge separated. It appears that as far as charge separation is concerned these two effects cancel each other out as the temperature is decreased from 20 to 0 °C.

(*e*) *Effect of applied electric fields*

It has been pointed out already that the application of an electric field in the region of a splash can change dramatically the charge separated by the splash. In this section we present more detailed measurements on this effect and interpret the observations theoretically.

Figure 27 shows the mean charge left on a copper sphere by the splashing of drops (2.5 mm in diameter) of dilute sodium chloride (2×10^{-4} mol l^{-1}) for various values of the applied electric field and for four different values of impact speed. In addition to demonstrating the increase in charge separation with increase in applied electric field the results show that, in the presence of an electric field of a given magnitude, as the speed of impact is increased from 1.5 to 4.1 m s^{-1} the charges separated increase but a further increase in the impact speed from 4.1 to 5.9 m s^{-1} decreases the charge separation. It can be seen from figure 28 that in the presence of applied electric fields the charge separation reaches a maximum for impact speeds around 3.5 to 4.5 m s^{-1}.

The charge separation was zero when no fragments were ejected from the crown formed by the splash. In the case of drops of diameter 2.94 mm this occurred when the impact speed fell

PHILOSOPHICAL TRANSACTIONS OF THE ROYAL SOCIETY A MATHEMATICAL, PHYSICAL & ENGINEERING SCIENCES

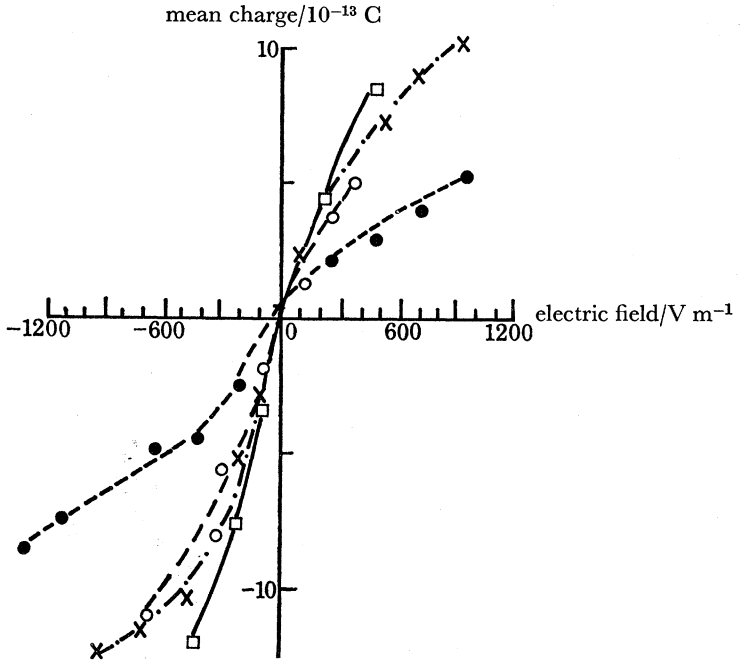

FIGURE 27. The effect of an applied electric field on mean charges transferred to a copper sphere at 20 °C by the splashing of drops 2.5 mm in diameter containing 2×10^{-4} mol l^{-1} of sodium chloride, at impact speeds of (○) 1.5, (□) 4.1, (×) 5.4 and (●) 5.9 m s^{-1}.

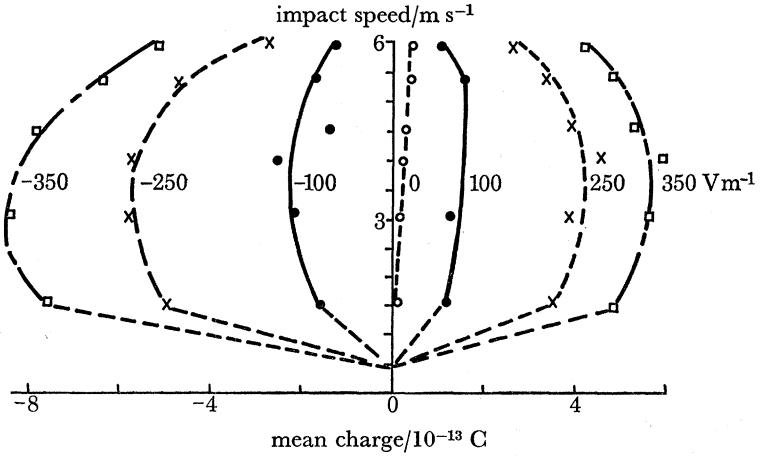

FIGURE 28. Mean charges transferred to a copper sphere as a function of impact speed in the presence of various electric fields by the splashing of drops 2.5 mm in diameter containing 2×10^{-4} mol l^{-1} of sodium chloride.

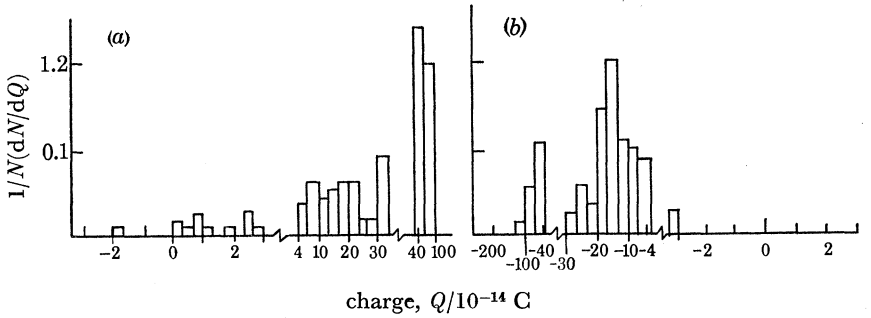

FIGURE 29. Normalized distribution of the charges transferred to a copper sphere when drops, 2.5 mm in diameter and containing 2×10^{-4} mol l^{-1} of sodium chloride, impacted on the sphere with a speed of 4.1 m s^{-1} in the presence of (*a*) a downward directed electric field of 230 V m^{-1} and (*b*) an upward directed electric field of 230 V m^{-1}.

below 0.4 m s^{-1}. The dashed lines in figure 28 represent extrapolations to an approximate impact speed below which no charges were separated by the splashes.

Figure 29 (*a*) is a normalized histogram of the charges left on a copper sphere after drops, 2.5 mm in diameter and containing 2×10^{-4} mol l^{-1} of sodium chloride, had splashed on it in the presence of a positive (i.e. downward directed) electric field of 230 V m^{-1}. In this case most of the charges were positive. Figure 29 (*b*) is the corresponding histogram when a negative electric field of 230 V m^{-1} was applied. In this case all of the charges were negative.

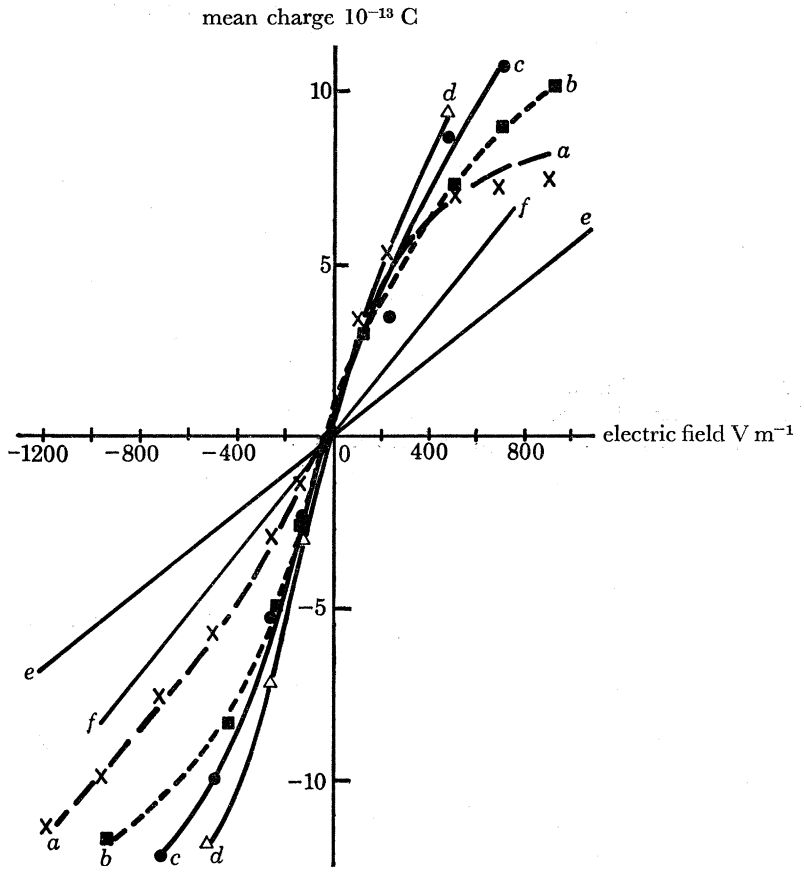

FIGURE 30. Mean charges transferred to a copper sphere due to the splashing of drops of pure water (electrical conductivity 12 μS m^{-1}) and dilute sodium chloride solutions (electrical conductivity 2.8 mS m^{-1}) in the presence of applied electrical fields. (*a*) pure water, impact speed 5.4 m s^{-1}, (*b*) sodium chloride solution, impact speed 5.4 m s^{-1}, (*c*) pure water, impact speed 4.1 m s^{-1}, (*d*) sodium chloride solution impact speed 4.1 m s^{-1}, (*e*) theoretical from equation (6), (*f*) theoretical from equation (8). Drops were 2.5 mm in diameter in all cases.

In figure 30 a comparison is made between the charges left on a copper sphere due to the splashing of pure water and dilute solutions of sodium chloride. The charges separated by the pure water are generally smaller in numerical magnitude than those separated by the sodium chloride solutions under the same conditions.

Polarization is undoubtedly responsible for the increase in the charge separated by a splash when an electric field is applied. A positive electric field will polarize the incoming drop and the target so that their upper and lower halves have net negative and positive charges respectively and during contact positive charge will be transferred from the drop to the target. A further

polarization will occur during the growth of the crown in such a way that the upper portions of the crown will carry a net negative charge and the lower portions a net positive charge. Consequently, in the absence of other effects, in the presence of an applied positive electric field the fragments produced by a splash will carry negative charges and in a negative electric field they will carry positive charges as observed experimentally. Gordon (see Latham & Mason 1962) has shown that in the case of two rigid and perfectly conducting spheres of radii R and r ($R > r$) which collide and separate in an electric field E, the total charge Q_s carried off by the larger sphere is given by

$$Q_s = \gamma_1 E r^2 \cos\theta + \frac{Q}{1+\gamma_2(r^2/R^2)}, \tag{6}$$

where, γ_1 and γ_2 are weak functions of r/R, θ is the angle between the electric field E and the lines of centres of the two spheres during contact, and Q is the original charge carried by the larger sphere. Curve (e) in figure 30 shows the values of Q_s calculated from (6) for the case of a drop of diameter 2.5 mm with no initial charge ($Q = 0$) which collides and rebounds from a larger sphere ($R \gg r$), θ has been taken as 45°. The theoretical curve is in surprisingly good agreement with the experimental measurements shown in figure 30. However, the application of (6) to splashing is obviously not strictly correct; some of the shortcomings of this approach are considered below.

Equation (6) applies to conducting spheres. This assumption will be valid for charge separation during the splashing of a water drop only if the relaxation time of the charge carriers is short compared to the time of ejection of the fragments. The relaxation time τ_R is given approximately by

$$\tau_R = D\epsilon_0/\kappa, \tag{7}$$

where, D and κ are the dielectric constant and the electrical conductivity of the drop, and ϵ_0 the permittivity of free space. For the drops used in our experiments κ varied from 10^{-5} to 10^{-3} S m^{-1}. For a solution drop $D = D_0 + 2\delta c$, where D_0 is the dielectric constant of pure water, c the molar concentration of the solution and for sodium chloride $\delta = 5.5$ (Robinson & Stokes 1959). For $c = 10^{-5}$ mol l^{-1}, $D \simeq D_0$. Hence, τ_R varied from 7×10^{-5} s (for pure water) to 7×10^{-7} s (for the aqueous solutions). For an impact speed of 4 m s^{-1}, the average time for the ejection of the initial fragments from the crown is of the order 10^{-4} s. Therefore, some of the fragments will have a contact time of the order of the relaxation time for pure water, and greater than the relaxation time for the aqueous solutions. Consequently, the assumption of a conducting sphere is incorrect for pure water and it may be questionable for the aqueous solutions when the speed of impact is high. The fact that the sphere cannot be considered as a good conductor will reduce the amount of charge Q_s below that predicted by (6).

Another important assumption leading to (6) is that the two spheres are rigid. However, we have seen that in a splash a crown forms from which charged fragments are ejected. As a result of this effect alone, the charges separated in a splash would tend to be greater than predicted by (6) because the capacitances of many fragments is greater than that of a single rebounding drop and also there will be a significant enhancement of the electric field near the highly curved surface of a fragment.

To allow for the above effects we write (6) in the form

$$Q_s = \sum_{n=1}^{n} \gamma_{1n} E_n r_n^2 \cos\theta_n \left[1 - \exp\left(\tau_{cn}/\tau_R\right)\right] + \sum_{n=1}^{n} \frac{Q}{1+\gamma_{2n}(r_n^2/R^2)} \tag{8}$$

where, n is the number of fragments (assumed spherical) of radius $r_1, r_2 \ldots r_n$, E_n is the local electric field near fragment n as it breaks away from the crown, θ_n the angle between the

PHILOSOPHICAL TRANSACTIONS OF THE ROYAL SOCIETY A MATHEMATICAL, PHYSICAL & ENGINEERING SCIENCES

direction of E_n and the line of contact between the nth fragment and the crown, and τ_{cn} is the contact time between the crown and the nth fragment.

In the light of the above discussion we can attempt to interpret the experimental results on the effects of applied electric fields on the charge separation by splashing. Figure 27 shows the effect of an applied electric field on the mean charge left on a copper sphere by the splashing of drops for four different speeds of impact. The drops consisted of a solution of 2×10^{-4} mol l^{-1} of sodium chloride which had an electrical conductivity of 2.8 mS m^{-1}. The relaxation time τ_R was therefore about 10^{-6} s. The mean charge separated by a splash increased rapidly as the electric field was increased, however, for a given electric field, the mean charge increased with increasing impact speed up to about 4 m s^{-1}, but as the speed of impact was increased above this value the mean charge decreased (figure 28). These results confirm the idea that the relaxation time is of the same order of magnitude as the contact time, and that when the contact time is decreased below a certain critical value (owing to an increase in the speed of impact) there will be a reduction in the mean charge separated by a splash. It appears therefore that for drops 2.5 mm in diameter the average contact time of the fragments with the crown is greater than the relaxation time for speeds of impact less than 4 to 5 m s^{-1}, but the reverse holds for high impact speeds.

We have seen (figure 30) that in the presence of an electric field there is a tendency for the mean charge separated by a splash to be greater for sodium chloride solutions than for pure water. This supports the argument that the higher the electrical conductivity of a drop the more charge is separated when splashing occurs in the presence of an electric field.

The fact that the theoretical curve (e) in figure 30 predicts much lower charges than those observed experimentally implies that the larger number of fragments which are produced by splashing (rather than the simple rebound assumed in (6)), and the enhancement of the local electric fields by the fragments, have a greater affect on the charging than does the fact that the drops cannot be considered perfect conductors. Curve (f) in figure 30 shows results obtained from (8) when it is assumed that the drop has no initial charge ($Q = 0$), the fragments consist of 100 droplets of equal size (60 μm) ejected at an angle $\theta_n = 45°$, $\tau_{cn} = \tau_R$, and $E_n = 10\,E$. It can be seen that in this case the theoretical curve lies closer to the experimental results than does (6).

It should be noted that the charges separated in a splash in the presence of an electric field reside primarily on the larger fragments ejected from the crown rather than the very small fragments which carry most of the charge in the absence of an applied field. This is because the contact time of the smaller fragments is much less than that of the larger fragments, and the enhancement which they cause in the local electric field due to their higher curvature is not sufficient to overcome their smaller surface area which has the dominant effect in equation (6).

4. Applications to charge separation in the atmosphere

4.1. *Splashing on solid hydrometeors in clouds*

In the region of natural clouds just below the 0 °C isotherm, water drops and large melting ice particles (hailstones, graupel, etc) can coexist. Collisions between these particles should result in splashing and the separation of charge as described in this paper.

If there is initially no electric field present in the cloud, the small liquid fragments produced by a water drop splashing on a melting ice particle should carry predominantly negative charges leaving the ice particle with a positive charge. If an updraught exists in the cloud, the gravitational separation of the small fragments and the large ice particles will result in the build-

up of a negative atmospheric electric field. Once such an electric field is created, the charge separation resulting from further collisions between water drops and ice particles will be dominated by the induction mechanism. In a negative electric field this will increase the positive charge received by the ice particle. Hence, a positive feedback mechanism will operate in which the charges separated by splashing will increase as the electric field increases. The magnitudes of the charges separated by this mechanism are quite sufficient to explain the region of positive charge which is often observed just below the freezing level in thunderclouds (Simpson & Robinson 1940). It is also interesting to note that the splashing of drops in clouds will result in the production of large numbers of small droplets and hence intrude upon the development of the spectrum of cloud droplet sizes. Berry (1967) has shown theoretically that starting with a narrow cloud drop size distribution (produced by condensation) growth by coalescence will produce a bi-model distribution in the size of the cloud droplets. However, relatively few droplets with radii about 40 μm result from the coalescence mechanism. Splashing provides a mechanism by which droplets of this size can be formed. Further growth of these small droplets by coalescence can lead to raindrops.

4.2. *Splashing of raindrops on the ground and over the ocean*

It has already been mentioned that Lenard observed a large concentration of negative space charge near waterfalls. This observation has been confirmed by Pierce & Whitson (1965). Negative space charge near the ground during heavy rain has been reported by Adkins (1959) who suggested that the fragments produced by the splashing of the raindrops on the ground might be responsible for this effect.

If we assume a logarithmic wind profile near the ground and an eddy viscosity K_m proportional to height Z then Bagnold (1941) has shown that

$$K_m = k_0 u_* (Z + Z_0), \tag{9}$$

where, k_0 is von Karman's constant ($= 0.4$), Z_0 is the roughness height, and u_* the frictional velocity. If we further assume that under steady state conditions the gravitational settling of the small fragments produced by raindrops splashing on the ground is just balanced by their upward turbulent transfer, then

$$ws = K_s(\partial s/\partial z), \tag{10}$$

where, w is the settling velocity, s the concentration of fragments in the air, and K_s the eddy diffusivity. If, as is often done, we take $K_m = K_s$ then from equations (9) and (10) we obtain

$$s = s_1(Z/Z_1)^{w/k_0 u_*} \tag{11}$$

where the subscript 1 refers to any reference level.

In order to estimate the effectiveness of this process in suspending the liquid fragments from the splashing of raindrops in the air we will consider a simple example. For a rainfall rate of 1 mm min^{-1} consisting of uniform drops 2 mm in diameter falling at their terminal velocity of 7 m s^{-1}, 10^{-3} m^3 of water will reach the ground in 1 min from 420 m^3 of air (i.e. 2.4 g of water per cubic metre of air). Since the mass of each drop is 4.2 mg, 2.4 g of water is equivalent to 570 raindrops. We will assume that the fragments ejected by a raindrop when it splashes on the ground follows a log–normal size distribution similar to that observed in the splashing of a drop in the laboratory, namely, 11.5 droplets 20 μm in diameter, 21 droplets 40 μm in diameter, 18.5 droplets 80 μm in diameter, 16.5 droplets 120 μm in diameter, 13.5 droplets 160 μm in diameter, 9 droplets 200 μm in diameter, 6 droplets 240 μm in diameter, and

4 droplets 280 μm in diameter. We will also assume that $u_* = 0.53$ m s^{-1} and $Z_0 = 0.05$ cm, which are the values found by Summerfeld & Businger (1965) for snow particles in the air.

With the above assumptions equation (11) gives the results shown as curves (*a*), (*b*) and (*c*) in figure 31. It can be seen from these results that small droplets are readily suspended in the air by turbulence, however, droplets greater than about 80 μm in diameter are difficult to suspend by this mechanism. However, Businger (1965) has shown that for the larger particles in blowing snow $K_s \neq K_m$. Solving (9) and (10) for such a case, we obtain

$$s = s_1(Z/Z_1)^{wK_m/K_s k_0 u_*}. \tag{12}$$

Curve (*d*) in figure 31 shows the results predicted by (12) for droplets 80 μm in diameter when $K_s = 1.3K_m$. This shows the effectiveness of increasing the value of K_s in suspending larger droplets.

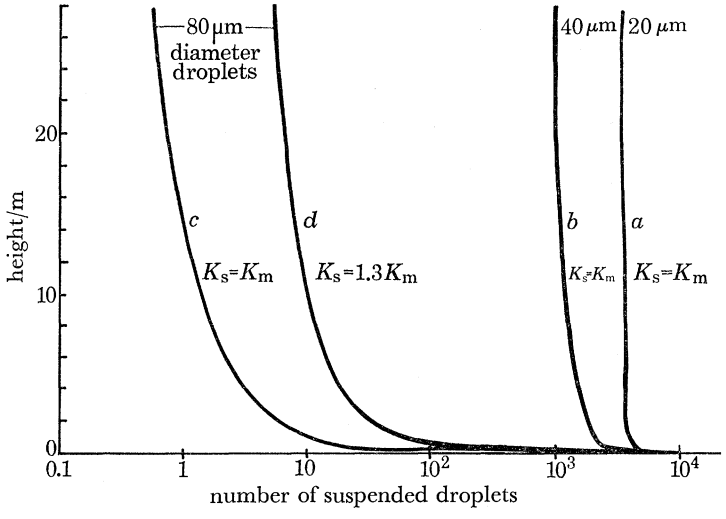

FIGURE 31. The suspension of droplets in the air ejected from the splashing of raindrops on the ground. Curves (*a*), (*b*) and (*c*) were calculated from equation (11) and curve (*d*) from equation (12).

Finally, it is interesting to speculate on the effects of raindrops splashing on the oceans. In this case the liquid in the crown comes mainly from the target liquid. Hence, due to the high concentration of sodium chloride in sea water, the streaming currents may initially be the dominant mechanism for separating charges during the break-up of the jets (see §3.1). In this case, the droplets ejected from the crown would carry a net positive charge into the air. However, after a long period of heavy rain a layer of fresh rainwater accumulates at the surface of the ocean (Katsaros 1969) so the splashing of raindrops into this layer would result in the ejection of negatively charged particles into the air.

We wish to thank Dr W. D. Scott for help during the course of this work. This research was supported by Grants GA-11250 and GA-17381 from the Atmospheric Sciences Section of the National Science Foundation. While the paper was being written one of us (P. V. H.) was on leave of absence at the Scott Polar Research Institute, Cambridge, England, and the other (Z. L.) was with the Department of Meteorology, U.C.L.A., Los Angeles, California. This is contribution no. 235 from the Atmospheric Sciences Department, University of Washington.

References

Adkins, C. J. 1959 *Q. Jl R. met. Soc.* **85**, 237.
Alty, T. 1924 *Proc. Roy. Soc. Lond.* A **103**, 316.
Alty, T. 1926 *Proc. Roy. Soc. Lond.* A **112**, 235.
Atkinson, W. R. & Paluch, I. 1966 *J. geophys. Res.* **71**, 3811.
Bach, N. & Gilman, A. 1938 *Acta phys.-chim. URSS* **9**, 1.
Bagnold, R. A. 1941 *The physics of blown sand and desert dunes*. London: Methuen.
Berry, E. X. 1967 *J. atmos. Sci.* **24**, 688.
Blanchard, D. C. 1963 *Progress in oceanography*, 1. Pergamon Press.
Bowden, F. P. 1966 *Phil. Trans. Roy. Soc. Lond.* A **260**, 94.
Bowden, F. P. & Brunton, J. H. 1967 *Proc. Roy. Soc. Lond.* A **263**, 433.
Bowden, F. P. & Field, J. E. 1964 *Proc. Roy. Soc. Lond.* A **282**, 331.
Businger, J. A. 1965 *J. geophys. res.* **70**, 3307.
Coehn, A. & Mozer, H. 1914 *Ann. Phys.* **43**, 1048.
Chapman, S. 1938*a* *Phys. Rev.* **54**, 520.
Chapman, S. 1938*b* *Phys. Rev.* **54**, 528.
Engel, O. G. 1955 *J. Res. natn. Bur. Stand.* **54**, 281.
Frumkin, A. & Obrutschewa, A. 1931 *Kolloid Z.* **54**, 2.
Gouy, P. M. 1910 *J. Phys.* **9**, 457.
Herden, G. 1960 *Small particle statistics*, London: Butterworth.
Heymann, F. J. 1969 *J. appl. Phys.* **40**, 5113.
Hobbs, P. V. & Osheroff, T. 1967 *Science, N.Y.* **158**, 1184.
Iribarne, J. V. & Mason, B. J. 1967 *Trans. Faraday Soc.* **63**, 2234.
Jonas, P. R. 1968 Ph.D. Thesis, University of London, England.
Jonas, P. R. & Mason, B. J. 1968 *Trans. Faraday Soc.* **64**, 547.
Katsoros, B. C. 1969 Ph.D. Thesis, University of Washington, Seattle, Washington.
Latham, J. & Mason, B. J. 1961 *Proc. Roy. Soc. Lond.* A **260**, 523.
Latham, J. & Mason, B. J. 1962 *Proc. Roy. Soc. Lond.* A **266**, 387.
Lenard, P. 1892 *Ann. Phys.* **46**, 584.
Lenard, P. 1915 *Ann. Phys.* **47**, 463.
Macklin, W. C. & Hobbs, P. V. 1969 *Science, N.Y.* **166**, 107.
Nolan, J. J. & Enright, J. 1922 *Proc. Roy. Dublin Soc.* **17**, 1.
Pierce, E. T. & Whitson, B. L. 1965 *J. atmos. Sci.* **22**, 314.
Prandtl, Von L. 1932 *Beitr. Phys. frei. Atmos.* **19**, 188.
Pruppacher, H. R., Steinberger, E. H. & Wong, T. L. 1969 *Planetary electrodynamics*. New York: Gordon & Beach.
Rayleigh, Lord 1879 *Proc. Roy. Soc. Lond.* **29**, 71.
Riel, K. & Hallett, J. 1968 *Rev. Scient. Instrum.* **40**, 533.
Robinson, R. A. & Stokes, R. H. 1959 *Electrolyte solutions*. London: Butterworth.
Rupe, J. H. 1950 *Rep. Jet. Prof. Lab.* California Institute of Technology.
Savic, P. & Boult, G. T. 1955 *Nat. Res. Lab. Canada*, Report MT-26.
Scott, W. D. & Levin, Z. 1970 *J. atmos. Sci.* **27**, 463.
Simpson, G. C. & Robinson, G. D. 1940 *Proc. Roy. Soc. Lond.* A **177**, 281.
Summerfeld, R. & Businger, J. A. 1965 *J. geophys. Res.* **70**, 3303.
Taylor, G. I. 1959*a* *Proc. Roy. Soc. Lond.* A **253**, 296.
Taylor, G. I. 1959*b* *Proc. Roy. Soc. Lond.* A **253**, 313.
Taylor, G. I. 1959*c* *Proc. Roy. Soc. Lond.* A **253**, 296.
Thompson, J. J. 1894 *Phil. Mag.* **37**, 341.
Workman, E. J. & Reynolds, S. E. 1950 *Phys. Rev.* **78**, 254.
Worthington, A. M. 1876 *Proc. Roy. Soc. Lond.* **25**, 261.
Worthington, A. M. 1877 *Proc. Roy. Soc. Lond.* **25**, 498.
Worthington, A. M. & Cole, R. S. 1897 *Phil. Trans. Roy. Soc. Lond.* A **180**, 137.
Worthington, A. M. & Cole, R. S. 1900 *Phil. Trans. Roy. Soc. Lond.* A **194**, 175.

PHILOSOPHICAL TRANSACTIONS OF THE ROYAL SOCIETY A MATHEMATICAL, PHYSICAL & ENGINEERING SCIENCES

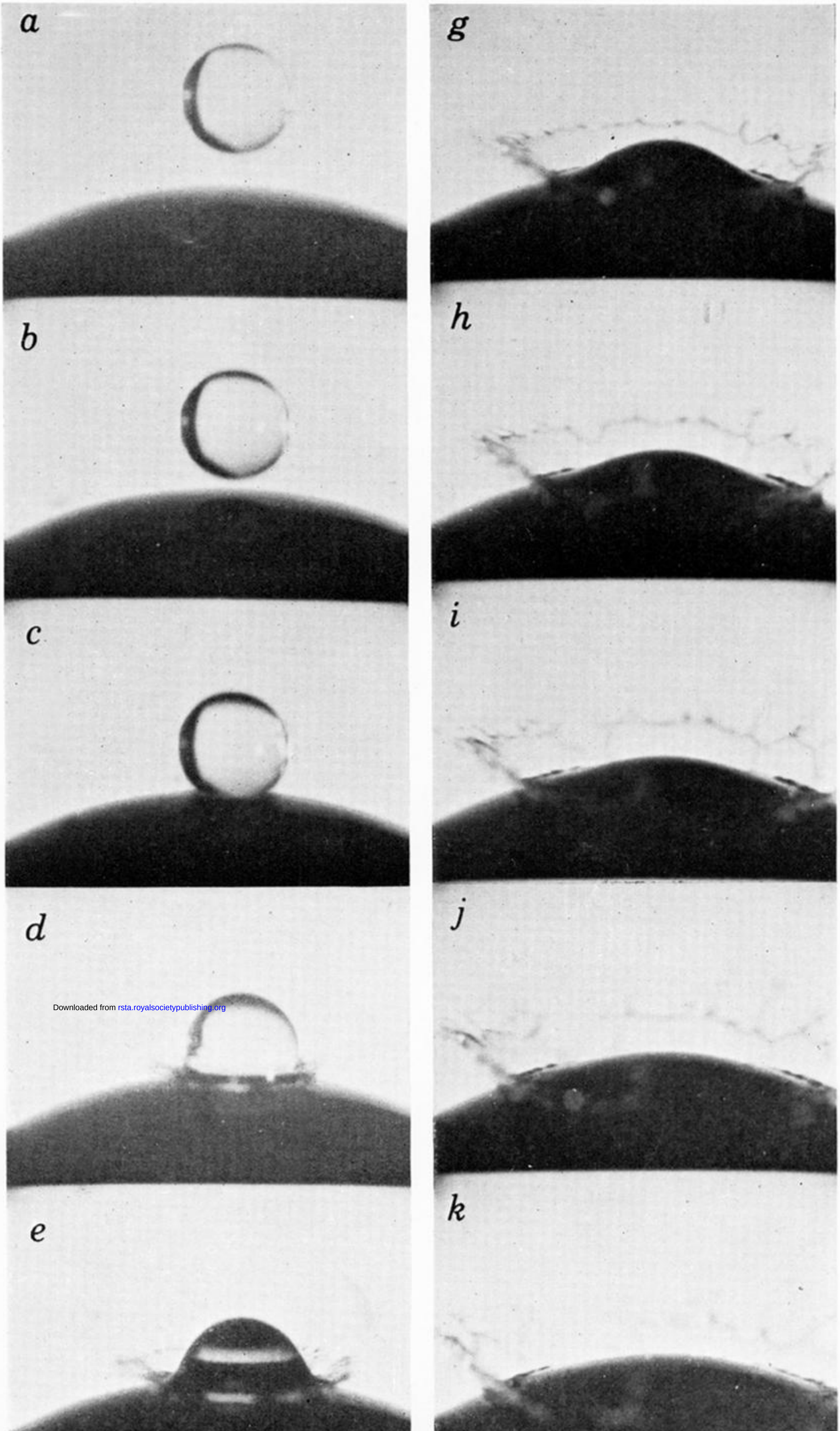

FIGURE 2. For legend see facing page

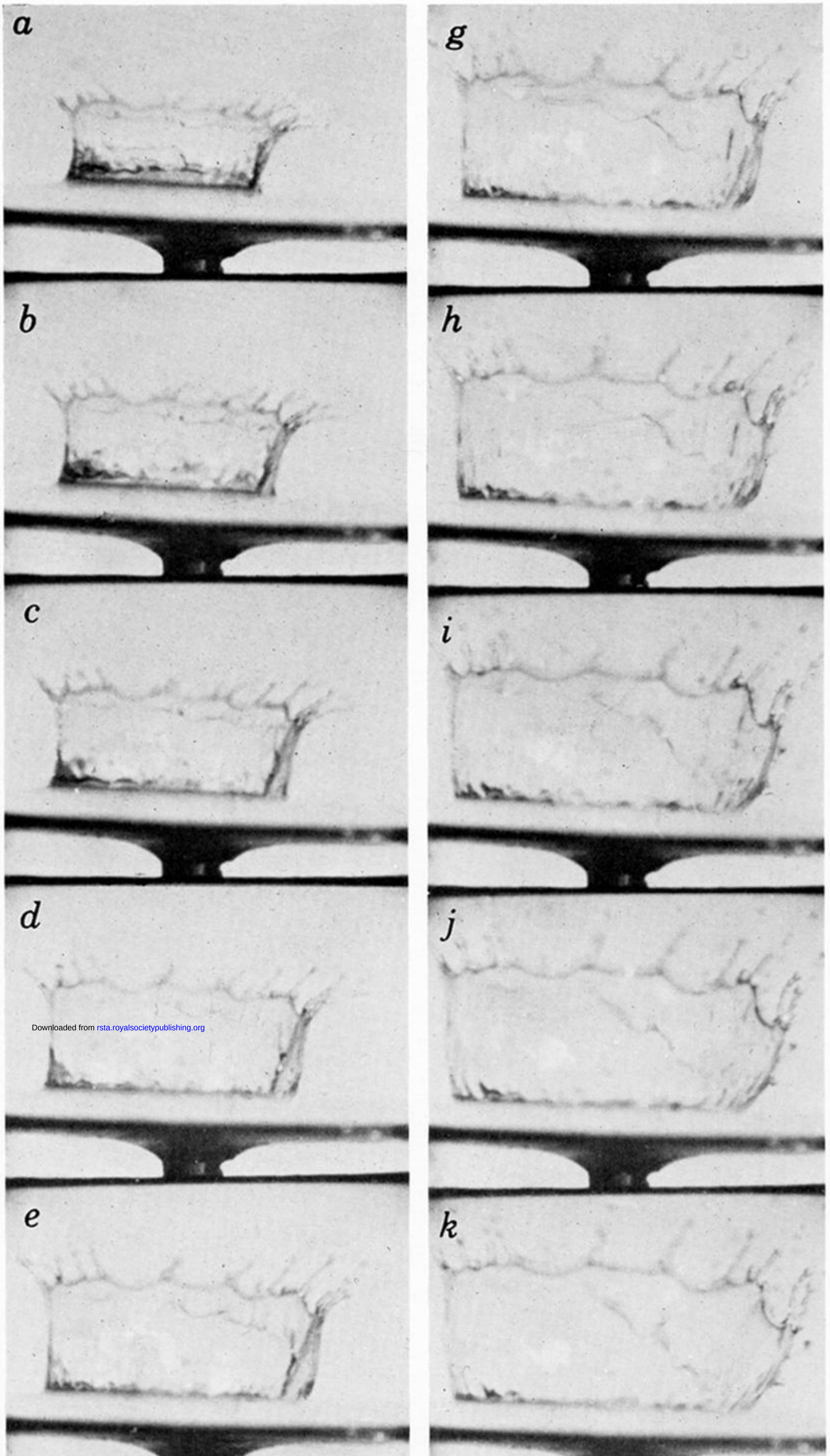

t = 1 ms 1.2 1.4 1.6 1.8 2.0 2.2 2.4 2.6 2.8 3.0 3.2

FIGURE 8. For legend see facing page

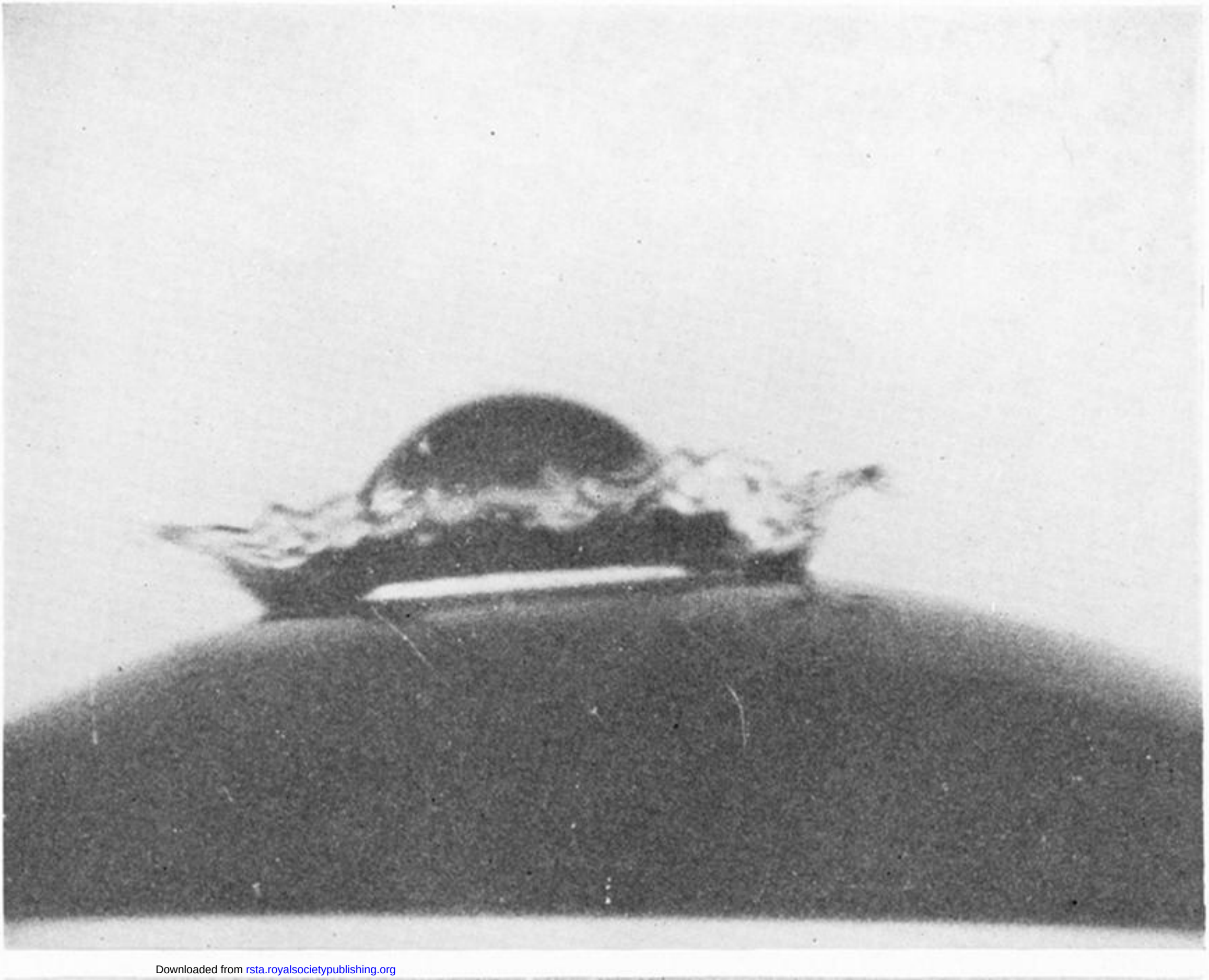

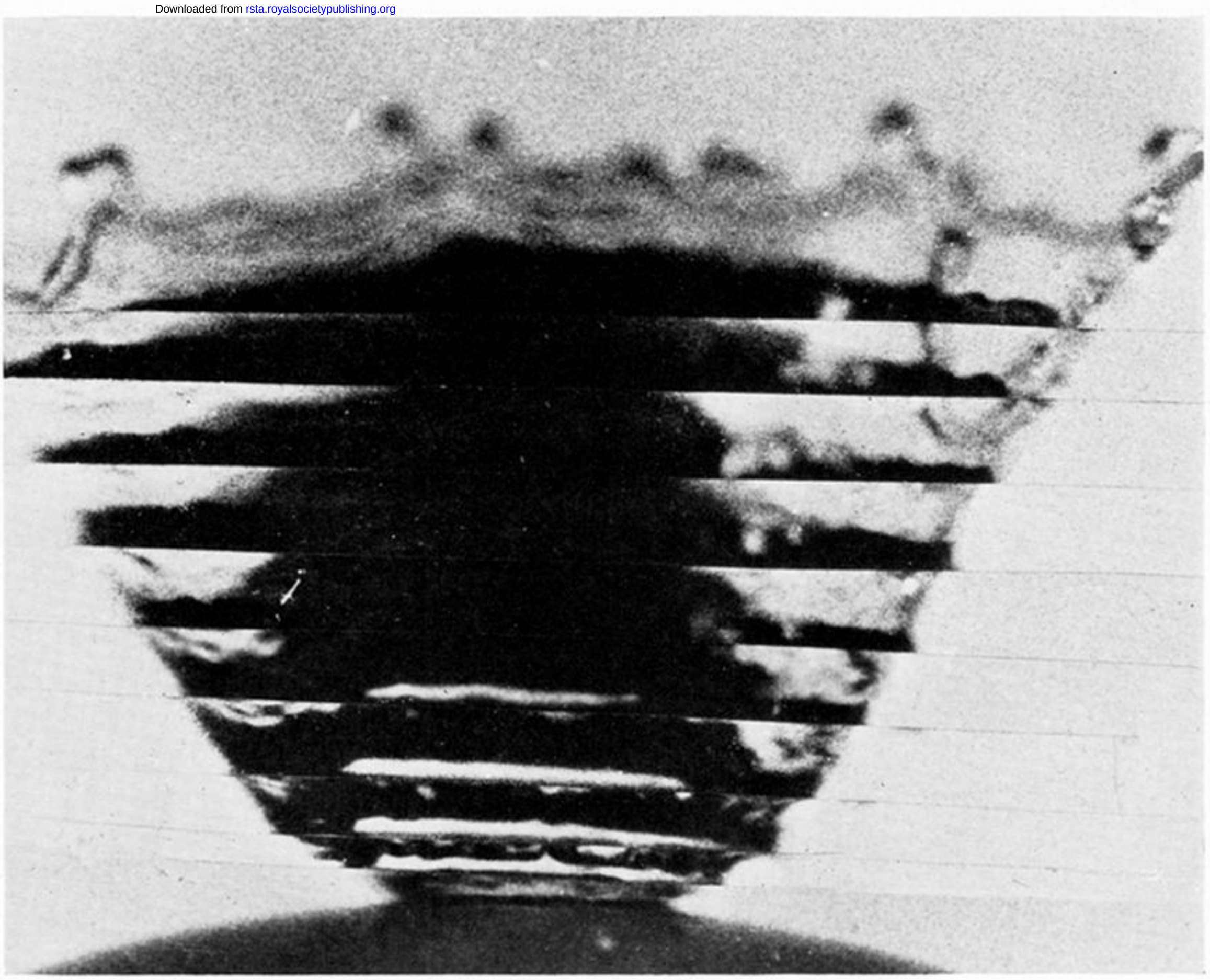

FIGURE 11. Symmetrical waves on the wall of the crown viewed with transmitted light. (Magn. × 11.5.)

FIGURE 12. Composite photograph illustrating the growth of the crown.

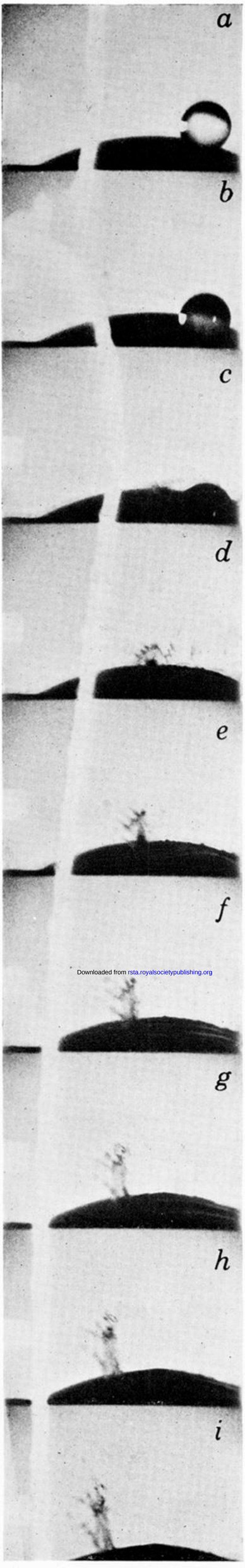

17

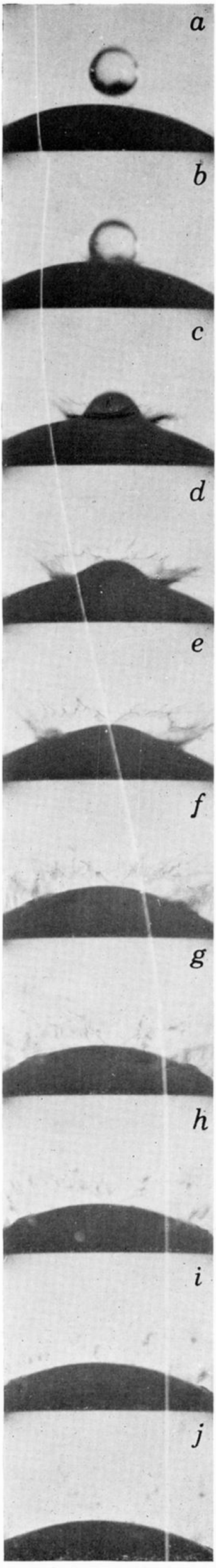

19

PHILOSOPHICAL TRANSACTIONS OF THE ROYAL SOCIETY A MATHEMATICAL, PHYSICAL & ENGINEERING SCIENCES

FIGURES 17 and 19. For legends see facing page